USGS
science for a changing world

Prepared in cooperation with the Alaska Department of Transportation and Public Facilities

Streambed Scour Evaluations and Conditions at Selected Bridge Sites, Alaska, 2016–17

Scientific Investigations Report 2019-5110
Version 1.1, April 2023

U.S. Department of the Interior
U.S. Geological Survey

Cover: U.S. Geological Survey hydrologic technician conducting bathymetric survey of Ward Creek beneath Bridge 747 near Ketchikan, Alaska. (Photograph taken by Robin Beebee, U.S. Geological Survey.)

Streambed Scour Evaluations and Conditions at Selected Bridge Sites, Alaska, 2016–17

By Robin A. Beebee, Karenth L. Dworsky, and Schyler J. Knopp

Prepared in cooperation with the Alaska Department of Transportation and Public Facilities

Scientific Investigations Report 2019-5110
Version 1.1, April 2023

U.S. Department of the Interior
U.S. Geological Survey

U.S. Department of the Interior
DAVID BERNHARDT, Secretary

U.S. Geological Survey
James F. Reilly II, Director

U.S. Geological Survey, Reston, Virginia
First release: 2019
Revision: April 2023, ver. 1.1

Suggested citation:
Beebee, R.A., Dworsky, K.L., and Knopp, S.J., 2019, Streambed scour evaluations and conditions at selected bridge Sites in Alaska, 2016–17 (version 1.1, April 2023): U.S. Geological Survey Scientific Investigations Report 2019-5110, 32 p., https://doi.org/10.3133/sir20195110.

Associated data for this publication:
Beebee, R.A., Knopp, S.J., Dworsky, K.L., and Schauer, P.V., 2019, Tabular input/output data and model files for 19 hydraulic models for streambed scour evaluations at selected bridge sites, Alaska, 2016–17: U.S. Geological Survey data release, https://doi.org/10.5066/P9LUTFHZ.

ISSN 2328-0328 (online)

Contents

Figures

Tables

Conversion Factors

U.S. customary units to International System of Units

Multiply	By	To obtain
	Length	
inch (in.)	2.54	centimeter (cm)
inch (in.)	25.4	millimeter (mm)
foot (ft)	0.3048	meter (m)
mile (mi)	1.609	kilometer (km)
	Area	
square mile (mi^2)	259.0	hectare (ha)
square mile (mi^2)	2.590	square kilometer (km^2)
	Flow rate	
foot per second (ft/s)	0.3048	meter per second (m/s)
square foot per second (ft^2/s)	0.0929	square meter per second (m^2/s)
cubic foot per second (ft^3/s)	0.02832	cubic meter per second (m^3/s)
	Acceleration	
foot per square second (ft/s^2)	0.3048	meter per square second (m/s^2)

International System of Units to U.S. customary units

Multiply	By	To obtain
	Length	
millimeter (mm)	0.03937	inch (in.)

Temperature in degrees Fahrenheit (°F) may be converted to degrees Celsius (°C) as:

$$°C = (°F - 32) / 1.8.$$

Datums

Vertical coordinate information is site specific and, in most cases, is referenced either to as-built elevations on bridge plans (if available) or to a reference mark with an assumed elevation of 100 feet established during the survey on or near the bridge deck. Other geographic data (for example, lidar) are adjusted to match the bridge datum, unless otherwise noted.

Horizontal coordinate information is referenced to the World Geodetic System of 1984 (WGS 84).

Abbreviations

ADCP	acoustic Doppler current profiler
ADOT&PF	Alaska Department of Transportation and Public Facilities
AEP	annual exceedance probability
EMA	Expected Moments Algorithm
FEMA	Federal Emergency Management Agency
HEC-RAS	Hydrologic Engineering Center River Analysis System
lidar	light detection and ranging
SRH-2D	Sediment and River Hydraulics Two-dimensional Model
USGS	U.S. Geological Survey

Streambed Scour Evaluations and Conditions at Selected Bridge Sites, Alaska, 2016–17

By Robin A. Beebee, Karenth L. Dworsky, and Schyler J. Knopp

Abstract

Stream stability, flood frequency, and streambed scour potential were evaluated at 20 Alaskan river- and stream-spanning bridges lacking a quantitative scour analysis or having unknown foundation details. Three of the bridges had been assessed shortly before the study described in this report but were re-assessed using different methods or data. Channel instability related to mining may affect scour at one site, while channel instability related to flow distribution changes can be seen at one site. One bridge was closed because of abutment scour prior to the study. Otherwise, channels generally showed stable bed elevations.

Contraction and abutment scour were calculated for all 20 bridges, and pier scour was calculated for the 2 bridges that had piers. Vertical contraction (pressure flow) scour was calculated for one site at which the modeled water surface was higher than the superstructure of the bridge. Hydraulic variables for the scour calculations were derived from one-dimensional and two-dimensional hydraulic models of the 1- and 0.2-percent annual exceedance probability floods (also known as the 100- and 500-year floods, respectively). Scour also was calculated for large recorded floods at two sites.

At many sites, overflow of road approaches relieves the bridge during floods and lessens the potential for scour. Two-dimensional hydraulic models are superior to one-dimensional hydraulic models at distributing flow between bridges, road approaches, and floodplains, and therefore likely produce more reasonable scour values at sites with substantial floodplain flow.

Introduction

Bridge foundations, including abutments and piers, depend on being embedded a certain depth into the streambed for stability. The required embedment depth varies with bridge and foundation type, soil properties, and seismic conditions. Bridge scour refers to the removal of streambed material beneath a bridge (fig. 1), generally by hydraulic stresses exerted on the streambed and bridge foundation during floods. Scour has the potential to damage bridges by undermining or destabilizing the bridge foundation and is the leading cause of bridge failure in the United States (Lagasse and others, 2012). In 1988, the Federal Highway Administration established a policy that all bridges be assessed for scour potential (U.S. Department of Transportation, 1988). It is standard engineering practice for bridge engineers to evaluate scour potential during the design process and to plan foundations accordingly. However, a national inventory of bridges and engineering plans indicated that numerous bridges in Alaska lacked quantitative scour assessments and (or) detailed foundation information needed to categorize the vulnerability of the structure to damage or failure by scour. Some of these bridges are old and plans have been lost, some were emergency replacements after floods, and others were intended to be temporary structures. A hydraulic assessment of streambed scour potential is needed in every case. The Alaska Department of Transportation and Public Facilities (ADOT&PF) intends to use these assessments to prioritize for further investigation those sites determined to have a high potential for streambed scour. The U.S. Geological Survey (USGS) has been studying scour at Alaskan bridges since 1964 (Norman, 1975), in cooperation with the ADOT&PF. In 1994, the USGS began a phased process to provide hydraulic assessments of scour for more than 400 bridges throughout Alaska (Heinrichs and others, 2001; Conaway, 2004; Conaway and Schauer, 2012; Beebee and Schauer, 2015; Beebee and others, 2017).

Scour is primarily a symptom of an undersized or misaligned bridge, and its severity depends on the magnitude of flood events that occur in the reach and the extent to which a bridge is blocking flow paths during floods. Other factors include the mobility of streambed material, embankment stability, debris accumulation, channel stability, and upstream sediment supply. Standard quantitative engineering methods do not account for every riverine process that influences scour (Conaway, 2007), and these methods have typically been applied using an assumption of one-dimensional flow because it is efficient to simulate using models. However, field conditions rarely exhibit one-dimensional flow characteristics.

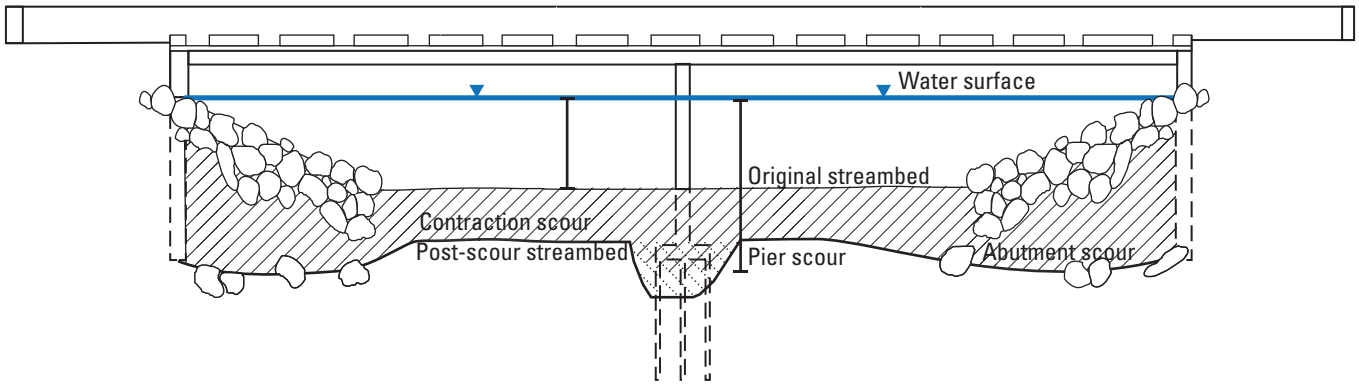

Figure 1. Example of streambed scour around a bridge foundation.

The error produced by one-dimensional assumptions varies by site geometry and flow level. For these assessments, two-dimensional models are used at 20 sites. Three of the two-dimensional modeling sites were previously assessed using one-dimensional models (Beebee and others, 2017).

The 20 sites selected by ADOT&PF for scour assessments are located primarily in Southcentral Alaska in different geographic and hydrologic settings (table 1; fig. 2).

Study Approach

The approach to assessing stability and scour at existing bridges includes components of geomorphology, flood history and frequency, and hydraulics:

1. Stream stability and geomorphology assessment generally following the methods of Lagasse and others (2012);
2. Flood history and flood frequency (design flood) estimates following the methods of Curran and others (2016);
3. Hydraulic model development and scour calculations following the guidance of Arneson and others (2012) and Shan and others (2016). Types of scour addressed include channel-wide scour caused by contraction of the channel width through the bridge and local scour around piers and abutments.

Stream Stability and Geomorphic Assessment

Arneson and others (2012) recommended that a general assessment of stream stability, aggradation, or degradation be done at bridges following guidelines in Lagasse and others (2012) as a first step in a scour assessment. Many streams in Alaska are naturally unstable because of high gradient, large glacial sediment supply, a lack of containment, freeze-up and breakup, or relatively frequent overbank floods. Some also have been either destabilized or stabilized by human activity, such as in-stream mining and urbanization. These factors may influence the vulnerability of structures and embankments to scour and erosion. The general geomorphic setting of each stream channel in this study was determined using aerial photographs, topographic data from light detection and ranging (lidar), ADOT&PF bridge inspection reports, and on-site assessments by USGS personnel. Stream stability was classified qualitatively based on evidence of channel change, active sediment sources, and human disturbance (excluding the bridge) as “stable,” “less stable,” and “unstable.” The qualitative classification takes both vertical and lateral instability into account. A quantitative classification derived from sounding records takes only vertical instability into account. Since 1998, ADOT&PF has taken biannual soundings (distance-from-bridge measurements) on the upstream side of bridges in conjunction with bridge inspections to look for changes in streambed elevation. The USGS took soundings on the upstream and downstream sides of bridges for this study. Because ADOT&PF inspectors and USGS personnel typically took depth measurements at different locations along the bridge face and used slightly different techniques, only the minimum bed elevation was compared between surveys done by the different agencies. The average change in minimum bed elevation between successive soundings (1–2 years apart) was used to look for evidence of channel aggradation or degradation, and the maximum change from the highest minimum bed elevation and the lowest minimum bed elevation was used to determine relative vertical stream stability. Divisions in relative stream stability categories were based on natural breaks in the data. Stream size determines changes in bed elevation to some extent (Lagasse and others, 2012). To compare differently sized streams, elevation changes were normalized by the extent of the wetted channel width of the modeled 100-year flood at the bridge opening.

Table 1. Descriptions of selected bridge sites evaluated for scour in Alaska, 2016–17.

[**NBI Code 113:** The National Bridge Scour Critical code for bridge. **Abbreviations**: ft, foot; T, bridge over tidal waterways with no scour analysis; U, bridge with unknown foundations and no scour analysis; WGS 84, World Geodetic System of 1984; 6, bridge with no scour analyses]

Bridge No.	River or stream	Latitude (WGS 84)	Longitude (WGS 84)	Year built	NBI Item 113 Code	Bridge length (ft)
1712	Cottonwood Creek	61.610	−149.290	2013	6	62
2207	Cottonwood Creek	62.205	−150.475	2010	6	60
1709	Little Susitna River at Moose Meadows	61.652	−149.431	2012	6	60
2225	Little Susitna River at Reed	61.666	−149.339	2016	6	88
1713	Little Susitna River at Welch Road	61.678	−149.313	1974	6	41
811	Livengood Creek	65.529	−148.544	1994	6	28
1985	Moose Creek	62.229	−150.443	1996	6	63
1018	North Fork Anchor River	59.778	−151.817	1965	6	43
812	Peters Creek	62.374	−150.738	1938	6	152
2226	Sawyer Creek	62.134	−150.020	2010	6	40
1199	South Fork Anchor River	61.224	−149.888	1966	U	72
1940	Ship Creek	59.702	−151.632	1992	6	134
2206	Twin Creek	62.190	−150.497	2010	6	41
747	Ward Creek	55.408	−131.715	1975	T	195
1708	Wasilla Creek	61.572	−149.309	2010	6	50
2227	Wasilla Creek	61.551	−149.294	2006	6	42
2238	Wasilla Creek	61.552	−149.316	2006	6	41
2286	Wasilla Creek	61.576	−149.284	2010	6	42
1782	Willow Creek	61.769	−149.954	2012	6	137
1831	Willow Creek	61.775	−149.910	1987	U	203

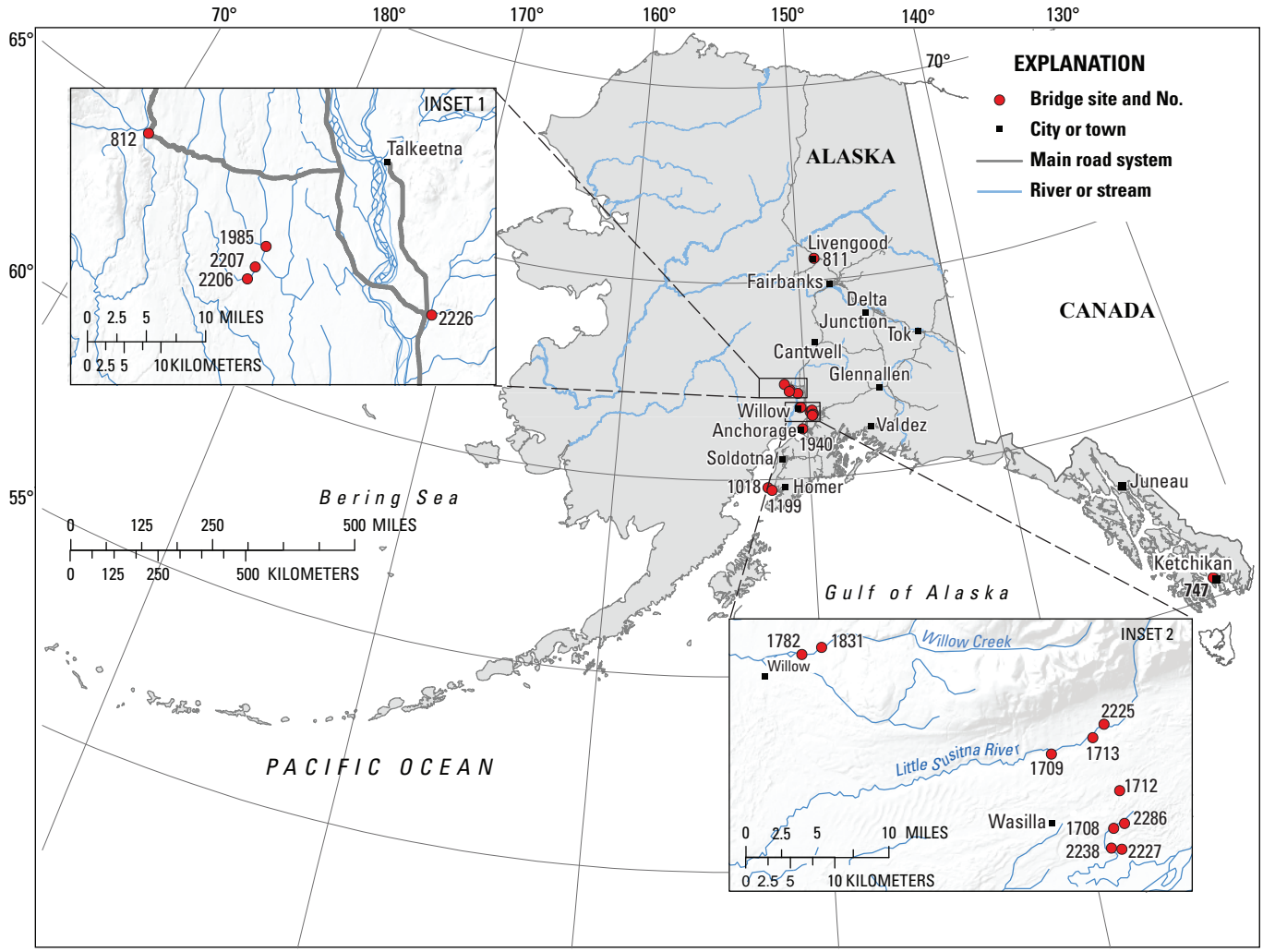

Base map from Alaska Department of Natural Resources (coastline, 1993, 2000; major rivers, 1998), Alaska Department of Transportation (major roads, 2007), Alaska Department of Natural Resources (towns,1998) World Geodetic System of 1984

Figure 2. Locations of selected bridge sites where scour was evaluated, Alaska.

Sites with less than ±0.4 foot (ft) of relative change per 10 ft of channel width between surveys were considered stable, sites with greater than or equal to ±0.4 ft and less than 0.8 ft of change per 10 ft of channel width were considered less stable, and sites with greater than or equal to ±0.8 ft of change in minimum bed elevation per 10 ft of channel width were considered unstable.

Stream Stability Results

Most channels had evidence of geomorphic or anthropogenic instability, and many had major changes in channel shape or flow distribution in the last decade (table 2; fig. 3). However, few sites showed much variation in streambed elevations in the sounding record (appendix 1). Only Livengood Creek 911 had bed elevation changes that met the unstable criteria. Both instream mining and a reported beaver dam breach upstream of the Livengood Creek bridge likely contributed to changes in streambed elevation. Of the three sites affected by changes in flow distribution on the Little Susitna River, one site was classified as less stable based on streambed elevation variation, though all three show major changes in bank and channel location. The large-scale migration of the main channel at the Willow Creek bridges likewise was not accompanied by large changes in streambed elevation. Instream engineering work created channel changes seen at Sawyer Creek where the bridge was replaced and North Fork Anchor River where the channel was rerouted and stabilized. Instability seen at Ward Creek 747 is located mid-channel and may be related to scour and fill during tidal cycles. Instability at Wasilla Creek Bridge 2227 may be related to a very mobile upper bed layer of silty sand overlying the gravel bed. All other sites were classified as stable based on the sounding record, with the caveat that many sites have short records.

Table 2. Stream stability as assessed using geomorphic evidence and repeat sounding records at selected bridge sites in Alaska.

[**Abbreviations**: ADOT&PF, Alaska Department of Transportation and Public Facilities; ft, foot; ft/10-ft-width, feet of relative change per 10 feet of width between]

Bridge No.	River or stream	Geomorphic setting	Natural sediment sources	Evidence of channel change	Human disturbance
1712	Cottonwood Creek	Lakes, low-gradient alluvium, groundwater fed	Minor, lake upstream	Channel split downstream, otherwise very minor	Residential area, household trash in stream, park upstream of bridge
2207	Cottonwood Creek	Low-gradient forested wetlands	Minor	Sharp bend upstream of bridge pushes flow into right bank, otherwise minor	Minor
1709	Little Susitna River at Moose Meadows	Forested braidplain below steep mountains	Minor; decomposing granite glacial till and outwash	Bank erosion, trees in river, flooded forest, changing flow distribution.	Low density residential area
2225	Little Susitna River at Reed	Forested braidplain below steep mountains	Minor; decomposing granite glacial till and outwash	Debris jams and floods have greatly affected flow distribution into this channel.	Residential area, yards adjacent to stream, local water withdrawal.
1713	Little Susitna River at Welch Road	Forested braidplain below steep mountains	Minor	On extensive, forested braidplain. Abandoned channels. Changing flow distribution.	Road embankments, yards, houses
811	Livengood Creek	Forested, incised channel	Minor	Beaver dam upstream occasionally breaches	Dredging, mining debris and trash in stream
1985	Moose Creek	Low-gradient forested wetlands	Minor	Meandering river. Oxbows visible upstream and downstream of bridge.	Low density residential area
1018	North Fork Anchor River	Forested braidplain	Minor	Abandoned channels, old meander cut-offs	Recent erosion control project, road embankments, yards, houses
812	Peters Creek	Low-gradient meandering floodplain	Minor	Minor: mostly straight, single channel river, with some anastomosis	Placer mining in headwaters, 16 miles upstream
2226	Sawyer Creek	Low-gradient forested wetlands	Minor, relict glacial outwash	Minor	Rural residential area
1199	South Fork Anchor River	Forested braidplain	Minor bank erosion.	Meander bend cut-offs	Minor
1940	Ship Creek	Incised, armored tidal channel	Tidal mud	Minor	Industrial area with bridges, trails, fishing access
2206	Twin Creek	Low-gradient forested wetlands	Minor	Minor abutment scour	Minor
747	Ward Creek	Bedrock-controlled tidal lagoon	Minor tidal gravel, lake and lagoon upstream	Substantial armoring on both banks upstream and downstream of bridge.	Residential and business area with a boat ramp directly downstream
1708	Wasilla Creek	Lakes, low-gradient alluvium, groundwater fed	Minor	Minor	Residential area set away from streambanks
2227	Wasilla Creek	Lakes, low-gradient alluvium, groundwater fed	Minor	Minor	Bank stabilization right around bridge
2238	Wasilla Creek	Lakes, low-gradient alluvium, groundwater fed	Minor	Minor	Residential area, yards adjacent to stream
2286	Wasilla Creek	Lakes, low-gradient alluvium, groundwater fed	Minor	Minor	Residential area on one side, yards adjacent to stream
1782	Willow Creek	Forested braidplain below steep mountains	Minor, relict glacial outwash	River has widened between 2011 and 2017 aerial photos. Main channel is concentrated on left bank and a large scour hole has developed along the left abutment and immediately upstream of bridge along the riprap reinforced left bank approach.	Creek passes through a dispersed residential area along this reach. Fishing. Boating
1831	Willow Creek	Forested braidplain below steep mountains	Minor, relict glacial outwash	2012 flood washed out right bank abutment. River has widened between 2011 and 2017 aerial photos.	Creek passes through a dispersed residential area along this reach. Fishing. Boating

Table 2. Stream stability as assessed using geomorphic evidence and repeat sounding records at selected bridge sites in Alaska.—Continued

Bridge No.	Qualitative geomorphic stability	Available soundings	Average low bed elevation change between site visits (ft)	Maximum low bed elevation change		100-year channel width (ft)	Adjusted bed elevation change (ft/10-ft-width)	Sounding-based stability assessment	ADOT&PF inspection notes
				Bed elevation change (ft)	Date range				
1712	Stable	2014–16 biennial	–0.1	0.3	2014–16	17.9	0.2	Stable	Bridge built in 2013
2207	Stable	2012–16 biennial	0.6	1.3	2012–16	45.0	0.3	Stable	Old bridge had flood damage, new bridge (2010) in good shape
1709	Less stable	2014–16 biennial	–0.2	0.9	2014–16	59.8	0.2	Stable	Changing flow distribution
2225	Unstable	2007–16	–0.4	2.8	2010–16	63.5	0.4	Less Stable	Changing flow distribution and bridge replaced in 2016
1713	Less stable	2012–4 biennial, 2013	0.3	0.5	2012–14	46.7	0.1	Stable	Changing flow distribution. Bridge replaced in 2011. Older bridge classified as less stable
811	Less stable	2000–16 biennial, 2009, 2011	–0.1	1.8	2001–05	22.6	0.8	Unstable	Beaver dam ouburst, debris, Inadequate riprap
1985	Less stable	2002–16 biennial	0.0	1.0	2002–04	65.3	0.2	Stable	2006 flood report indicates 5 ft of scour, not seen in soundings
1018	Stable	2001–11 biennial, 2012, 2013	0.2	2.3	2009–13	34.2	0.7	Less Stable	Bank erosion/undercutting, gabion failure
812	Less stable	2004–16 biennial	0.0	1.7	2008–10	133.0	0.1	Stable	Bank erosion. Left bank abutment erosion
2226	Stable	2012–16 biennial	0.4	2.2	2012–16	32.0	0.7	Less Stable	Bridge rebuilt in 2010.
1199	Stable	2001–13 biennial	–0.3	1.8	2003–13	71.2	0.3	Stable	Bank/abutment erosion, light debris
1940	Stable	2001–11 biennial, 2012, 2015, 2016	0.5	1.9	2009–15	116.4	0.2	Stable	Abutment erosion, contraction, channel moved from left to right side
2206	Stable	2012–16 biennial	–0.1	0.3	2012–16	34.8	0.1	Stable	Undercutting of abumtent caps, light drift, scour under bridge
747	Stable	2007–17 biennial, 2003, 2012	–0.3	3.9	2003–17	78.8	0.5	Less Stable	Undercutting and bank sloughing within 15 feet of both abutments.
1708	Stable	2010–16 biennial	–0.1	0.4	2016	34.5	0.1	Stable	Minor left bank upstream erosion
2227	Stable	2010–16 biennial	–0.2	1.5	2014–16	36.1	0.4	Less Stable	Erosion at both abutments
2238	Stable	2007, 2008, 2017	–0.1	0.4	2008–17	33.7	0.1	Stable	–
2286	Stable	2010–16 biennial	0.1	0.5	2012–16	38.4	0.1	Stable	–
1782	Less stable	2012–16 biennial	0.4	3.8	2014–16	109.5	0.3	Stable	Left bank sloughing DS of bridge, logs and debris build-up on NE side of bridge
1831	Less stable	2002–12 biennial, 2016	–0.6	3.6	2002–08	219.7	0.2	Stable	Scour at pier 4, fill loss around right abutment

Table 3. Hydraulic modeling input data and sources from selected bridges in Alaska.

[D_{50}: Median grain diameter. D_{95}: Grain diameter that is greater than 95 percent of the population. **Abbreviations**: ADCP, acoustic Doppler current profiler; DS, downstream; lidar, light detection and ranging; ft, foot; ft/ft, foot per foot; mm, millimeter; US, upstream; –, variables that were not used in analysis for that site]

Bridge No.	River or stream	Manning's roughness coeffcient for channels	US boundary condition slope (ft/ft)	DS boundary condition slope (ft/ft)	Boundary condition source	D_{50} (ft)	D_{84} (ft)	Grain size source	Channel geometry source	Overbank geometry
1712	Cottonwood	0.045	NA	0.023	Survey	0.105	0.17	Wolman count	Survey and soundings	Lidar[1]
2207	Cottonwood	0.045	NA	0.003	Survey	0.138	0.31	Image analysis	Survey and soundings	Lidar[1]
1709	Little Su at Moose Meadows	0.040	NA	0.004	Survey and lidar	0.131	0.22	Image analysis	Survey and soundings	Lidar[1]
2225	Little Su at Reed	0.045	NA	0.006	Survey and lidar	0.168	0.34	Image analysis	Survey and soundings	Lidar[1]
1713	Little Su at Welch	0.045	NA	0.010	Lidar	0.131	0.2	Wolman count	Survey and soundings	Lidar[1]
811	Livengood	0.055	0.02	0.02	Survey	0.110	0.26	Image analysis	Survey and soundings	Survey
1985	Moose Creek	0.050	NA	0.001	Lidar	0.100	0.24	Image analysis	Survey and soundings	Lidar[1]
1018	North Fork Anchor River	0.040	NA	0.007	Survey	0.099	0.2	Wolman count	Survey	Lidar[3]
812	Peters Creek	0.045	NA	0.002	Survey	0.100	0.24	Image analysis	Survey and soundings	Survey
2226	Sawyer Creek	0.045	NA	0.010	Lidar	0.100	0.25	Wolman count	Survey and soundings	Lidar[1]
1199	South Fork Anchor River	0.055	NA	0.002	Lidar	0.143	0.2	Wolman count	Survey and soundings	Lidar[3]
1940	Ship Creek	0.025	NA	0.005	Survey	0.112	0.17	Image analysis	Survey and soundings	Lidar[2]
2206	Twin Creek	0.045	NA	0.008	Survey and lidar	0.092	0.17	Image analysis	Survey and soundings	Lidar[1]
747	Ward Creek	0.035	NA	–[5]	Tidal elevations	0.105	0.17	Wolman count	Survey and soundings	Lidar[4]
1708	Wasilla Creek	0.045	NA	0.004	Survey and lidar	0.151	0.40	Image analysis	Survey and soundings	Lidar[1]
2227	Wasilla Creek	0.045	NA	0.002	Survey and lidar	0.002	0.00	Seive analysis	Survey and soundings	Lidar[1]
2238	Wasilla Creek	0.045	NA	0.010	Lidar and survey	0.151	0.24	Wolman count	Survey and soundings	Lidar[1]
2286	Wasilla Creek	0.045	NA	0.005	Survey and lidar	0.150	0.28	Wolman count	Survey and soundings	Lidar[1]
1782	Willow Creek	0.030	NA	0.004	Lidar	0.212	0.36	Image analysis	Survey and soundings	Lidar[1]
1831	Willow Creek	0.045	NA	0.006	Lidar	0.270	0.51	Image analysis	Survey and soundings	Lidar[1]

[1]2011 Matanuska-Susitna Lidar.

[2]2018 Anchorage Lidar.

[3]2008 Kenai Peninsula Borough Lidar.

[4]2014 Ketchikan Borough Lidar.

[5]Downstream boundary is 4.1 ft, or mean lower low water elevation in as-built datum.

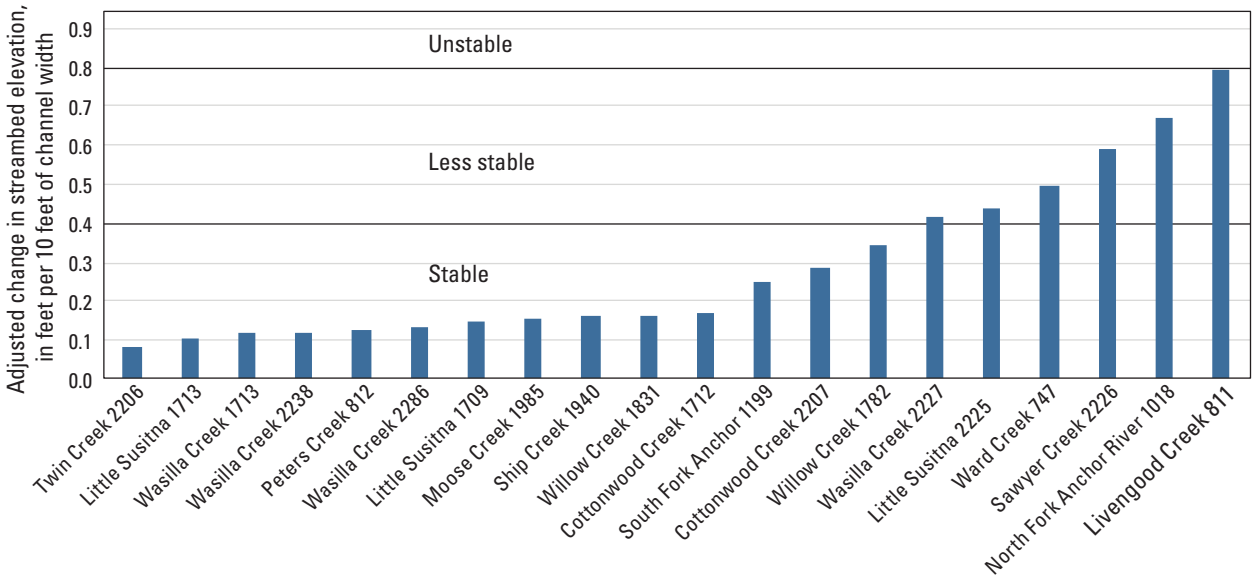

Figure 3. Sounding-based stream stability at bridge sites, Alaska.

The average change in minimum bed elevation between successive soundings was less than or equal to 0.5 ft at all sites except for Willow Creek Bridge 1831, which had an average of -0.6. The record indicates that the minimum bed elevation regularly increased and decreased by several feet between soundings, with no consistent trend toward degradation. No physical evidence of aggradation or degradation (incised channels or alluvial fan formation) was observed during field visits.

Repeat cross-section soundings are useful in identifying instabilities but cannot be used to rule out vulnerability to scour or other responses to flooding. Scour and fill often are short-lived and are evident only during and shortly after a flood (Conaway, 2007). Soundings taken at 2-year intervals, even if a flood occurs between soundings, may not indicate the transient effects of the flood on the channel cross section. Seven bridges have only 2–4 years of soundings (table 3). Short sounding records are less likely to capture long-term trends or responses to infrequent flood events. Additionally, nine bridges were replaced in the last 10 years, and bathymetry can change dramatically with the new bridge.

Flood History and Frequency Analysis

Standard engineering practice is to design bridges to safely withstand the hydraulic conditions encountered during large, rare floods, referred to as the “design flood” (Arneson and others, 2012). Scour at the bridge site also is calculated for even larger floods, known as the “check floods” or “super floods.” The design flood and check flood for Alaskan bridges typically are the 1- and 0.2-percent annual exceedance probability (AEP) floods (also referred to as “100- and 500-year recurrence interval floods”), respectively. The AEP is the probability that a select flow will be equaled or exceeded annually. For example, a 1-percent AEP flow has a 1-percent chance of being equaled or exceeded in any given year.

Statewide regression equations for Alaska developed by Curran and others (2016) were used to calculate 1- and 0.2-percent AEP flows at all sites (Q_{reg}). For 11 sites with continuous gages or crest-stage gages that were on the same stream but not co-located with the bridge, a station estimate (Q_{sta}) was also calculated using Bulletin 17C flood frequency methods (England and others, 2018) and PeakFQ version 7.0 software (Veilleux and others, 2013). The regression variables (drainage area and mean annual precipitation) used for each site and gaged period of record are shown in table 4**.** Symbols for each estimate follow Curran and others (2016) for consistency. Equations for each estimate are in Curran and others (2016).

Curran and others (2016) suggest that at sites on gaged streams with drainage areas from ½ to 1 ½ times the size of the drainage area of the gaged site, two regression estimates be used to weight the station estimate. This increases the statistical strength of the estimate because the regression is developed from many more data points than the station estimate. The station estimate Q_{sta} is first weighted by the regression estimate for the gaging station $Q_{(sta)reg}$, giving a weighted station estimate $Q_{(g)wtd}$, then $Q_{(g)wtd}$ is adjusted to the ungaged site by a drainage area ratio giving $Q_{(u)g}$, and lastly the adjusted value is weighted by the regression value for the ungaged site giving $Q_{(u)wtd}$. This technique was used at Ship Creek 1940 where the station and regression estimates were consistent. For the remaining 10 sites near gages, the station estimates deviated sharply from the regression estimates for physical process-based reasons. For these cases, the weighted station estimate was adjusted by drainage area, but not weighted a second time with the regression estimate at the bridge. For three bridges on the Little Susitna River, a model was used to distribute the design flow between subchannels.

Table 4. Variables used in the flood frequency analysis for selected bridges in Alaska.

[**Abbreviations**: in., inch ; mi², square mile; –, variables either are unavailable or are not used in flood frequency analysis]

Bridge No.	River or stream	Station No.	Period of record for peak streamflow analysis	Number of peaks	Drainage area (mi²)	Mean annual precipitation (in.)
1712	Cottonwood Creek	15286000	1949–55, 1999–2000	8	12.3	18.1
2207	Cottonwood Creek	NA	NA	NA	8.48	28.6
1709	Little Susitna River at Moose Meadows	15290000	1949–2016	68	100.9	39.1
2225	Little Susitna River at Reed	15290000	1949–2016	68	82.7	41.4
1713	Little Susitna River at Welch Road	15290000	1949–2016	68	76.0	42.3
811	Livengood Creek	NA	NA	NA	19.7	13.2
1018	North Fork Anchor River	NA	NA	NA	29.7	29
1985	Moose Creek	NA	NA	NA	49.4	37.9
812	Peters Creek	NA	NA	NA	99	44.1
2226	Sawyer Creek	NA	NA	NA	21	31.7
1199	South Fork Anchor River	NA	NA	NA	120.2	31
1940	Ship Creek	15276000	1947–2016	70	123.4	30.7
2206	Twin Creek	NA	NA	NA	9.12	29.4
747	Ward Creek	NA	NA	NA	18.7	157
1708	Wasilla Creek	15285200	1980–1987	8	40.4	20.8
2227	Wasilla Creek	15285200	1980–1987	8	45.6	20.2
2238	Wasilla Creek	15285200	1980–1987	8	45.3	21
2286	Wasilla Creek	15285200	1980–1987	8	38.6	21
1782	Willow Creek	15294005	1979–2016	32	169.4	38.2
1831	Willow Creek	15294005	1979–2016	32	167.8	38.4

Flood History and Frequency Results

Table 5 includes discharge measurements, estimates of the 1- and 0.2-percent AEP flows, and large historical floods. No flood greater than the estimated 1-percent AEP flow occurred at bridge sites with nearby gages during the gaged period of record, though Willow Creek sites experienced a flow of 97 percent of the 1-percent AEP flow in 1987. A large flood in 2012 affected most of the Southcentral Alaska sites as well. Little Susitna Bridge 2225 was replaced following the 2012 flood, while Willow Creek Bridge 1831 suffered abutment fill loss, leaving the abutment piles mid-flow, and was closed following the 2012 flood.

Flood Frequency Results Where the Station and Regression Values Differ

At Cottonwood Creek 1712 and all four Wasilla Creek sites, the Q_{sta} values are significantly lower than the Q_{reg} values based on the regression equations. These streams are mostly groundwater fed and rise from low-lying wetlands and ponds at the base of the Talkeetna mountains. This type of low-discharge stream is not well-represented by gaging stations in Alaska, thus the statewide regression values would be expected to overestimate peak flows here. The drainage area of Cottonwood Creek at Bridge 1712 is more than twice that of the gaged drainage basin (26.2 square miles compared to 12.6 for the gage). Curran and others (2016) suggest that only Q_{reg} be used here. However, because the station values are smaller by a factor of 10 than the regression values at the gage, despite the larger drainage area, it seems reasonable to give weight to the gaged values. At the Wasilla Creek gage, regression estimates are about five times the station estimate (fig. 4). All five of these sites are in low flood risk zones in the Matanuska-Susitna Borough Flood Study maps (Federal Emergency Management Agency, 2011). $Q_{(u)g}$ was used for the design flows.

Conversely, at both Willow Creek and Little Susitna River gages, the station values are higher by a factor of two than the regression values. These streams drain adjacent steep, well-integrated basins in the southern Talkeetna mountains. Both drainages likely overperform the average basins in the regression study in runoff speed and concentration. The gage is upstream of the bridges on both streams. Using the weighted values $Q_{(u)wtd}$ results in smaller flow estimates with larger downstream drainage areas, which does not physically make sense. At these five sites, $Q_{(u)g}$ was used for the design flows.

Table 5. Discharges used to estimate scour at selected bridge sites in Alaska.

[**Source of 1 and 0.2 percent AEP estimate**: From Curran others (2016). **Abbreviations**: AEP, annual exceedance probability; ft^3/s, cubic foot per second; NA, not applicable; $Q_{(u)g}$ weighted station estimate adjusted by drainage area; Q_{reg} regression estimate for ungaged site; $Q_{(u)wtd}$, weighted station estimate adjusted by drainage area and weighted by regression estimate for ungaged site; –, variables that were not used in analysis for that site]

Bridge No.	River or stream	Discharge measurement (ft^3/s)	1-percent AEP discharge (ft^3/s)	0.2-percent AEP discharge (ft^3/s)	Additional discharge (ft^3/s)	Year of additional discharge	Source of 1 and 0.2 percent AEP estimate
1712	Cottonwood Creek	6.7	90	130	NA	NA	$Q_{(u)g}$
2207	Cottonwood Creek	8.5	710	960	NA	NA	Q_{reg}
1709	Little Susitna River at Moose Meadows	252.5	10,360	13,940	NA	NA	$Q_{(u)g}$
2225	Little Susitna River at Reed	5.6	8,970	12,070	NA	NA	$Q_{(u)g}$
1713	Little Susitna River at Welch	78	8,970	12,070	NA	NA	$Q_{(u)g}$
811	Livengood Creek	33	720	1,000	NA	NA	Q_{reg}
1985	Moose Creek	291.5	3,180	4,130	NA	NA	Q_{reg}
1018	North Fork Anchor River	127	1,790	2,370	NA	NA	Q_{reg}
812	Peters Creek	464.3	5,940	7,560	NA	NA	Q_{reg}
2226	Sawyer Creek	16.2	1,480	1,970	NA	NA	Q_{reg}
1199	South Fork Anchor River	86	5,230	6,730	NA	NA	Q_{reg}
1940	Ship Creek	208.4	4,650	6,010	NA	NA	$Q_{(u)wtd}$
2206	Twin Creek	2.9	760	1,030	NA	NA	Q_{reg}
747	Ward Creek	NA	4,630	5,760	NA	NA	Q_{reg}
1708	Wasilla Creek	13.6	430	600	NA	NA	$Q_{(u)g}$
2227	Wasilla Creek	14.9	470	650	NA	NA	$Q_{(u)g}$
2286	Wasilla Creek	12.8	420	580	NA	NA	$Q_{(u)g}$
2238	Wasilla Creek	15.5	470	650	NA	NA	$Q_{(u)g}$
1782	Willow Creek	460	12,340	17,130	12,000	10-11-1987	$Q_{(u)g}$
1831	Willow Creek	411	12,250	17,010	12,000	10-11-1987	$Q_{(u)g}$

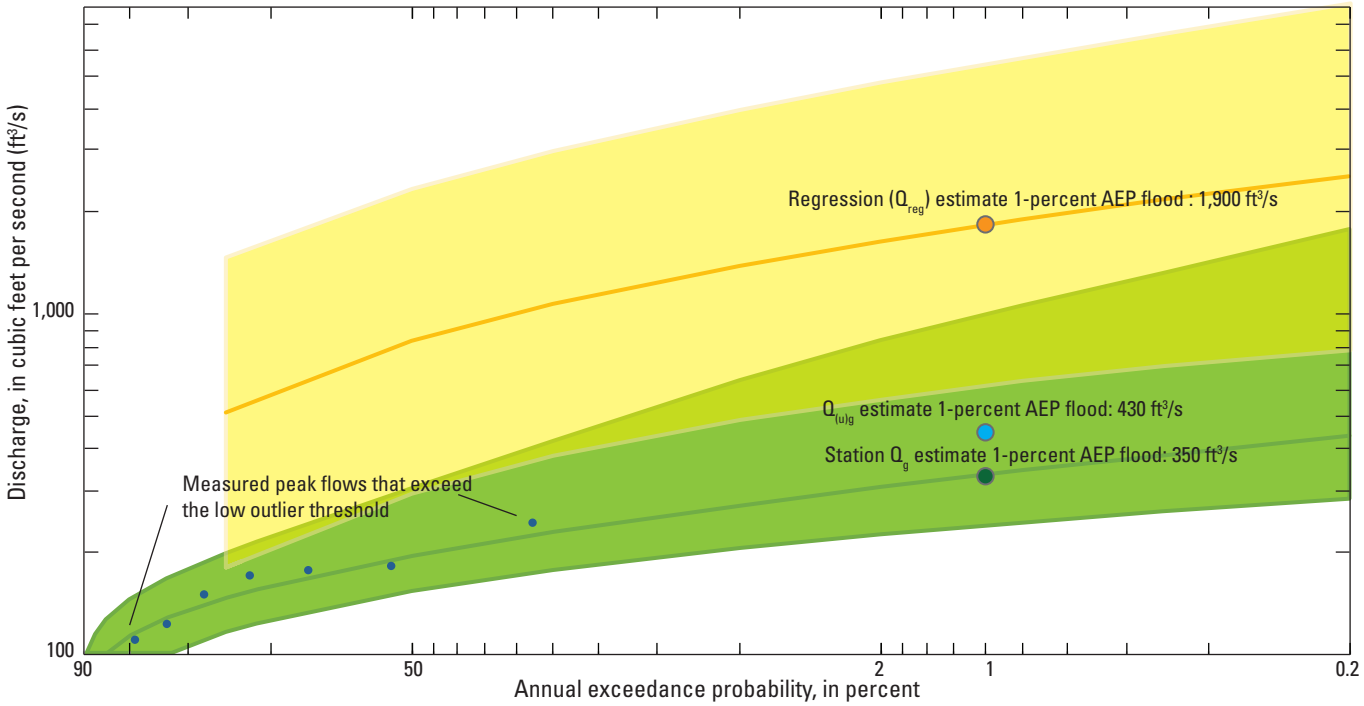

Figure 4. Expected Moments Algorithm station and regression analyses for the Wasilla Creek Gage (15285200), Alaska.

Hydraulic Model Development

In addition to flood flows, the basic data needed for a scour evaluation using a hydraulic model include:

1. Bridge geometry as measured in the field;
2. Channel and overbank elevations, including approach and exit cross sections located outside the expansion and contraction zone of the bridge and cross sections immediately upstream and downstream of the bridge;
3. Water-surface slope for boundary conditions (downstream for two-dimensional models, downstream and upstream for one-dimensional model);
4. Bed-material size;
5. An estimate of the channel and flood plain Manning's roughness coefficients (n); and
6. A discharge measurement for model calibration.

Elevation, grain size, and n data and sources for each site are listed in table 3. Two-dimensional and one-dimensional models have the same basic input requirements, except that two-dimensional models use a continuous grid of elevations and a computational mesh rather than separate cross-sections.

Stream Bathymetry, Topography, and Bridge Geometry Surveys

A datum point established at each site was used to determine relative elevations of the channel cross sections and bridge geometry. Streambed elevations were measured at the upstream and downstream face of each bridge using either sounding weights on cable reels, weighted measuring tapes, or acoustic Doppler current profilers (ADCPs), depending on the depth and current. Channel cross sections and water-surface slopes were surveyed with a total station. ADCPs were used to survey bathymetry in places where channels were too deep to wade. Bridge-deck elevation and slope, low-chord and high-chord elevations, bridge width, and the location and dimensions of piers and footings also were measured if construction plans provided insufficient information. Overbank areas were sometimes either inaccessible or too thickly vegetated to fully survey. In these cases, elevations derived from lidar supplemented the data for overbank geometry. Where stream gradients were low relative to errors in surveying, gradients were measured across a longer distance from lidar.

Discharge Measurements for Calibration

U.S. Geological Survey crews measured discharge with a current meter, Acoustic Doppler velocimeters, or ADCP, depending on the size of the stream following procedures in Turnipseed and Sauer (2010). Discharges were taken from the nearby gage for Willow Creek bridges 1782 and 1831. At Willow Creek Bridge 1831, velocity measurements were taken using an ADCP and used to help calibrate the model. All discharge measurements were obtained during low to moderate flow conditions. Discharge measurements are used to verify the channel roughness coefficient (n) that is used in the model. When discharges are very low compared to design flows, they are not useful for roughness calibration because they engage such a small percentage of the total channel geometry. Of the 20 sites, 8 had sufficient discharge to calibrate the channel roughness coefficient.

Grain-Size Analysis

Grain-size distribution, which is needed to check for cohesive behavior and live-bed or clear-water scour conditions and to calculate clear-water scour, was determined at all gravel-bedded sites using either a gravelometer or digital image analysis software (Bergendahl and Arneson, 2014). Streambed material at all sites was greater than the 0.2-millimeter median diameter grain-size (D_{50}) threshold for determining whether cohesion between grains would influence the scour process, thus only equations for cohesionless material were used. All sites were predominantly gravel-bedded.

Hydraulic Model Development

All scour calculations are based on hydraulic results from two-dimensional models rather than one-dimensional models. Two-dimensional models provide more accurate hydraulic results than one-dimensional models when cross-channel (two-dimensional) flow is likely to affect hydraulics at the bridge and channel approach sections. Scenarios with strongly two-dimensional flow include skewed bridges, contracted reaches, multiple channels, multiple bridges, and reaches where some flow is likely to cross the road approach rather than flow under the bridge (Zevenbergen and others, 2012; Burgess and others, 2016). Although most of the bridges in this study cross relatively small channels, they all exhibit one or more of these two-dimensional characteristics. The Bureau of Reclamation's Sediment and River Hydraulics two-dimensional Model (SRH-2D) (Lai, 2008) was used to calculate hydraulic variables. SRH-2D uses two-dimensional depth-averaged dynamic wave equations to compute flow profiles.

Models require four basic inputs to run: channel and floodplain geometry, flow, water-surface slope, and roughness coefficients for the channel and floodplain. For all study sites, cross-sections were surveyed at the upstream and downstream faces of the bridge to represent the contracted channel, and two to four additional cross-sections were surveyed upstream and downstream of the bridge to represent the uncontracted channel. The number of surveyed coordinates varied from 10 to 90 points per cross-section depending on channel size and method used. Floodplain elevations beyond the surveyed cross-sections were derived from lidar for all sites except for Livengood Creek, where all flow was contained in the channel, and Peters Creek, where lidar was not available and additional total station points were surveyed.

Channel and floodplain geometry were compiled from field surveys and lidar in a geographic information system, exported into text files with X, Y, and Z coordinates for each topographic point, and then compiled into a computational mesh in Surface-water Modeling System version 13.0 (SMS 13.0; Aquaveo, 2018). The mesh consists of triangular and quadrilateral elements. The channel and overbank points from different data sources were merged and smoothed in SMS. Channel survey data typically extended two bridge-lengths upstream and downstream of the bridge, which is sufficient for one-dimensional modeling. However, for two-dimensional modeling the boundary conditions were set at a contained part of the channel three or more bridge-lengths away from the bridge. To account for bathymetry outside of the extents of the survey data, either the closest cross-section was adjusted by slope and extrapolated along the channel to the model boundary, or a channel was cut into the lidar with the same average depth as the surveyed approach and exit cross-section. If the mesh between the surveyed cross-sections did not have sufficient resolution to match the aerial photos or other field observations, cross-sections were interpolated either by copying and adjusting by slope in ArcMap or by linear interpolation between cross-sections using HEC-RAS. The goal of such interpolation was to represent bends, gravel bars, and thalweg location near the bridge accurately in the computational mesh.

Because the number and size of mesh elements has a direct effect on computational time, attempts were made to reduce the number of mesh elements while preserving the resolution needed in the channel and bridge area. Typical lidar resolution is 3.5–8 ft. For larger model domains, mesh elements with 15–20 ft spacing were used along the floodplain boundaries and 5–10-ft spacing were used along the channels. For smaller model domains, 5–10-ft spacing was used throughout. The resulting meshes had from 3,000 to 650,000 elements, although the average was less than 100,000 elements. The model with the greatest number of elements encompassed Little Susitna Bridges 2225 and 1713, as well as several miles of upstream floodplain. The model domain started several miles upstream of the bridges where flow was mostly contained in one channel braid and needed sufficient resolution to distribute flow between braids and across the floodplain to estimate the fraction of flood flow that would approach each bridge.

Many of the study streams are braided or are set into a floodplain with relict braids. For larger floods, these overbank flow paths are important in routing floodwaters toward or away from structures and over roads. Breaklines were placed in the mesh along floodplain channel braids and linear structures such as roads to ensure that these flow paths were represented. Piers and vertical abutments were represented as voids in the mesh. Where the initial model runs indicated that the water surface may approach the low chord of the bridge, the bridge was added to the model as a pressure flow boundary condition.

All calibration discharges and floods were simulated as steady flows (in other words, with a single value rather than a hydrograph). All sites used normal depth for the downstream boundary conditions for floods. The water-surface slope that was surveyed at low water or the lidar derived water surface slope was used to determine normal depth.

Channel roughness varies with flow and channel location and represents a source of uncertainty in hydraulic models. Two-dimensional models account implicitly for roughness owing to cross-channel flow in meandering channels, an element that can account for up to 30 percent of n in traditional estimates for one-dimensional models (Arcement and Schneider, 1989). However, roughness elements owing to small-scale irregularities, vegetation, and bed material that are not captured in elevation data still must be estimated. Roughness coefficient values for the channel and overbanks were initially determined using visual methods following Chow (1959) and Hicks and Mason (1998). At the eight sites with moderate flow, surveyed water-surface elevations and measured velocities were compared to model simulation results and used to validate or refine channel roughness values (table 6). Ship Creek, Willow Creek 1831 and 1782, Little Susitna Bridges 1709 and 1713, Peters Creek, Moose Creek, and South Fork Anchor River two-dimensional models were calibrated using a discharge measurement at moderately low flow. At six of these sites, the water surface and velocities matched best with a n value of 0.04–0.055, comparable to visual comparison methods for small, gravel and cobble-bedded streams. The exceptions are Willow Creek 1782 and Ship Creek 1940, where n values of 0.03 and 0.025 best-matched velocity and water surface elevations. SRH-2D models were run with hydrograph time-steps from 1 to 2 seconds and for hydrograph durations ranging from 1 to 5 hours, depending on the length of modeled reach.

Little Susitna River Bridges 1709, 1713, and 2225 each cross relatively minor braids of the Little Susitna River downstream of USGS gage 1529000 (fig. 5). None of these braids have been gaged. The model domain for Bridge 1709 starts nearly a mile upstream of the bridge before flow splits so that the model could distribute flow between channels.

Likewise, a single model domain encompassing Bridges 1713 and 2225 starts 1.5 miles upstream of the bridge. The primary factor limiting the accuracy of the modeled flow splits is the changing nature of channel bathymetry and thus flow distribution over time. For very large floods, such as the 1-percent and 0.2-percent AEP flows, much of the flow is conveyed outside the main channels in the floodplain. Thus, changes in channel bathymetry have a smaller effect on the distribution of flow during design floods as compared to flows contained in the channel.

The recent history of Little Susitna River Bridges 2225 and 1713 illustrates the changing flow distribution on the Little Susitna River floodplain. Prior to 2006, flow was conveyed under the roadway by a 4-ft-diameter culvert at the current site of Bridge 2225. A large flood in 2006 (6,140 cubic feet per second [ft^3/s], the third highest peak on record) washed out the culvert and increased the size of the channel, until an estimated one-third of the Little Susitna River flow was conveyed through the new channel (HDR, Inc., 2006). A bridge was placed over the larger channel in 2006 and then was replaced in 2014. A larger flood in 2012 (7,740 ft^3/s, the second-highest peak on record) cut a new channel upstream of the flow split and left large piles of debris and gravel near the entrance to the 2225 channel, effectively restricting flow down the channel again. During the 2016 site survey, only 5.6 of 1,000 ft^3/s was flowing through Bridge 2225. Debris is mobile, however, and the channel could easily recapture a significant part of the Little Susitna River flow with the next flood. For this reason, the pre-2012 topography was used to route the design flood to Bridge 2225.

The 2012 flood greatly increased the size of the channel to Bridge 1713 on the Little Susitna River, as can be seen on aerial photos from 2011 and 2017 (fig. 6). To account for the increased area since the lidar was obtained, the topography was lowered by about 5 ft in the visible area of the 2017 channel to connect the main channel to the previously much smaller side channel leading to Bridge 1713. This creates a channel bed at the same elevation as the main channel bed.

Scour Calculations

Contraction and abutment scour were calculated for all sites using methods derived for streams with cohesionless sediments. Sediment transport conditions upstream of the bridge determined whether live-bed or clear-water contraction scour equations were used. A single abutment scour method that incorporates contraction scour was used for all sites to estimate total scour depth at each abutment. Pier scour was calculated using the Hager number/gradation coefficient equation following the recommendation of Shan and others (2016). Total scour at piers is calculated by adding pier scour to contraction scour. Neither site with piers had a notable debris accumulation problem, thus debris conditions were not modeled. All scour is calculated from the low bed elevation measured at the time of the survey; no adjustment was made for beds that had previously scoured.

Contraction Scour

Contraction scour can have horizontal and vertical components. Horizontal contraction scour is caused by road approach embankments and abutments in the flood plain or main channel that intercept flow and direct it through the bridge opening. Vertical contraction scour occurs when the superstructure of the bridge (girders, deck, curb, and railing) intercepts the water surface, creating pressure flow conditions. As flow accelerates through a smaller cross section, velocity and shear stress increase and transport streambed material downstream. As scour deepens a channel, cross-sectional area increases and shear stress and velocity decrease until scour reaches equilibrium depth (also referred to as the “depth of maximum scour”). Contraction scour is calculated and presented as a uniform lowering of the streambed across the channel cross section (fig. 7), but it rarely occurs uniformly because some areas of the streambed are more erodible than other areas, and flow is not evenly distributed across the channel. Contraction scour is calculated differently depending on the sediment transport properties of the approach channel and on whether pressure flow is present. All methods assume that the simulated flood lasts long enough to cause maximum scour and that the width of the contracted section remains constant and only depth increases until equilibrium depth is reached. In practice, erosion of embankments under a bridge often causes the channel to widen during a flood.

Clear-Water Compared with Live-Bed Contraction Scour

Contraction scour is calculated differently depending on whether the approach channel is transporting sediment into the bridge section (live-bed scour) or not (clear-water scour). For live-bed conditions, maximum scour depth is reached when sediment transported out of the bridge section equals the sediment transported in from the approach section. For clear-water conditions, maximum scour depth is reached when the shear stress in the bridge section decreases to the critical shear stress of the bed material in the section and sediment transport ceases. Live-bed or clear-water conditions for each simulated flow were determined by using equation 1 to compare the simulated velocity in the approach channel with the critical velocity necessary to transport the median grain size (D_{50}).

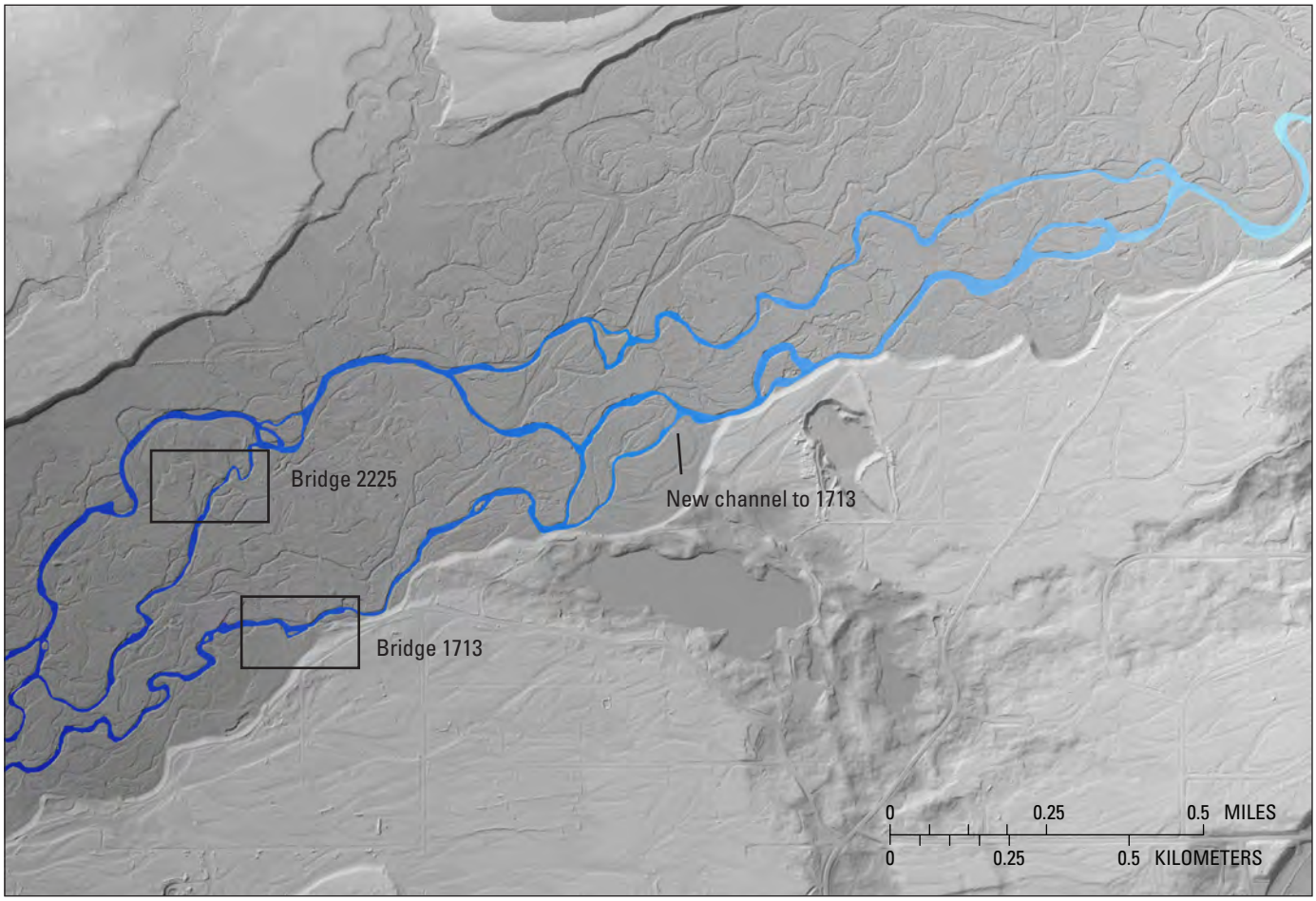

Figure 5. Little Susitna River and floodplain near bridges 1713 and 2225, Alaska, 2011. [Imagery by Matanuska-Susitna Borough]

Figure 6. Susitna River and floodplain at the entrance to Bridge 1713, Alaska, 2011 (*A*) and 2017 (*B*). [Imagery by Matanuska-Susitna Borough, Alaska]

Table 6. Manning's *n* calibration values for bridges with sufficient flow during measurement, Alaska.

[**Abbreviations**: ft, foot; ft/s, foot per second; *n*, Manning's roughness coefficient; –, variables that were not used in analysis for that site]

Bridge No.	River or stream	Calculated *n* from discharge measurement	Calibrated *n* from model	Survey water surface elevation (ft)				Model water surface elevation (ft)				Survey velocity (ft/s)	Model velocity	Average water surface difference (ft)	Average velocity difference (ft/s)
				1	2	3	4	1	2	3	4				
1709	Little Susitna at Moose Meadows	0.073	0.04	449.2	447.8	447.7	447.6	449.9	447.6	447.6	447.3	2.8	2.7	–0.0	0.1
1713	Little Susitna at Welch	0.087	0.045	555.9	555.7	555.7	555.1	556.0	555.4	555.4	555.1	1.3	1.6	0.1	–0.3
1985	Moose Creek	0.051	0.05	–	356.1	356.1	–	–	356.0	355.9	–	2.6	2.3	0.2	0.3
812	Peters Creek	0.041	0.045	89.7	88.2	88.2	86.4	89.4	87.8	87.7	86.5	2.5	2.7	0.3	–0.2
1940	Ship Creek	0.032	0.025	11.4	9.9	9.9	7.1	11.5	10.1	9.8	7.3	2.9	2.8	–0.1	0.1
1199	South Fork Anchor River	0.075	0.055	360.9	359.5	359.5	359.2	360.1	359.3	359.3	359.1	1.3	1.2	0.3	0.1
1782	Willow Creek	0.049	0.03	254.3	249.8	250.6	249.9	254.8	250.6	250.6	249.2	–	–	–0.1	–
1831	Willow Creek	0.058	0.045	343.5	–	333.6	332.1	343.6	–	333.6	332.5	3.3	3.3	–0.2	0.0

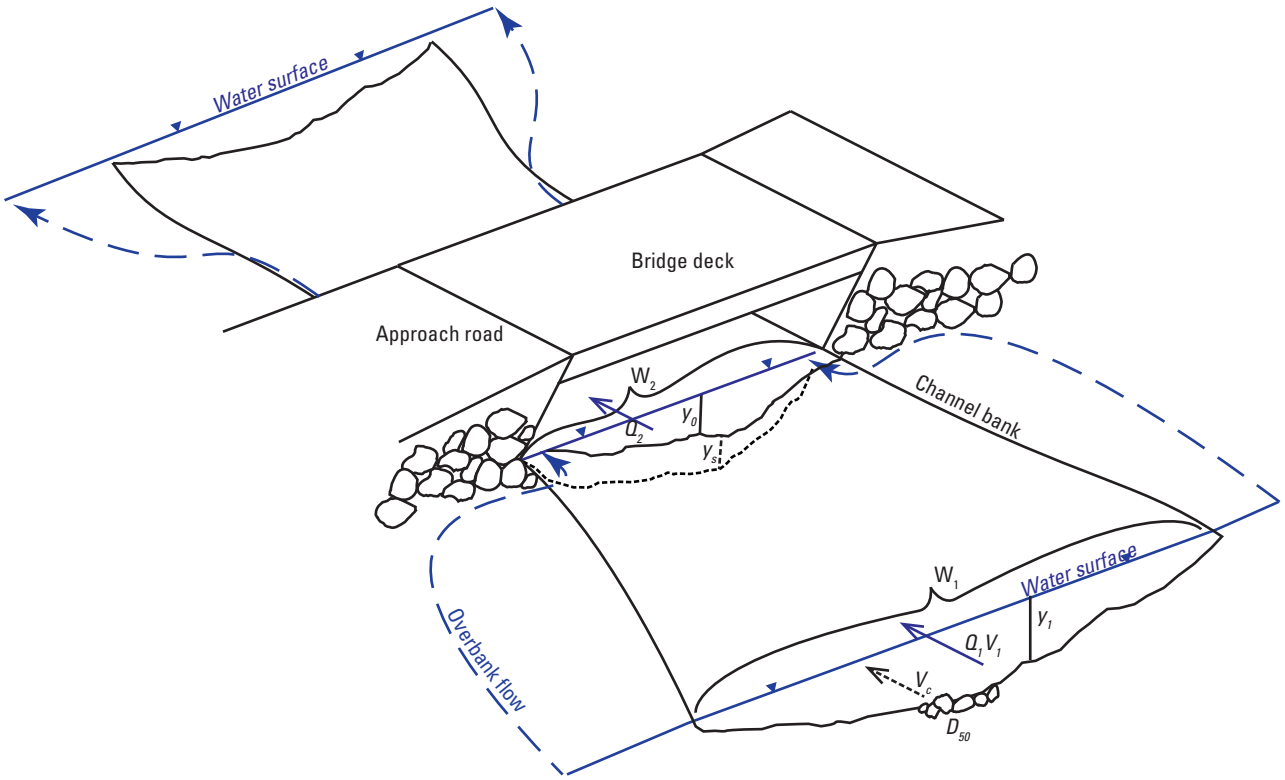

Figure 7. Basic contraction scour conditions and variables defined in equations 1–3.

$$V_c = 11.17 y^{1/6} D_{50}{}^{1/3} \quad (1)$$

where

V_c is the critical velocity above which D_{50} grain size and smaller will be transported, in ft/s;

y_1 is the average depth of flow upstream of the bridge, in ft; and

D_{50} is the median diameter of bed material, in ft.

A critical velocity map was constructed for each flood simulation using the depth for each model element (a triangular or quadrilateral cell representing a single computational point) and measured grain size. The critical velocity was subtracted from the calculated velocity at each element to construct a map showing where velocity exceeded the critical velocity threshold for sediment transport. This sediment transport map was used to determine live-bed and clear-water conditions, and to determine the width of flow transporting sediment for scour calculations. In cases of extreme backwater, such as those that occur when flow reaches the superstructure of the bridge, the velocity upstream of the bridge will drop below the critical velocity for sediment transport, and scour will change from a live-bed to a clear-water condition at the bridge (Arneson and others, 2012). This can cause conditions at a site to change from live-bed to clear-water between the design and check floods. This effect can be seen in the sediment transport map where critical velocity is exceeded everywhere along the reach except for a section upstream of the bridge.

Live-Bed Contraction Scour

Live-bed contraction scour is calculated using equation 2 (Arneson and others, 2012). The equation depends on the ratios of discharge and width between the approach section and the contracted section, as well as the depths in the approach section and contracted section. The live-bed equation will only estimate scour if there is a decrease in width and (or) an increase in discharge between the approach channel and the bridge section. Because it does not include grain size, the live-bed equation may overestimate actual scour when the contracted section is armored.

$$y_s = y_1 \left[\left(\frac{Q_2}{Q_1} \right)^{\frac{6}{7}} \left(\frac{W_1}{W_2} \right)^{k_1} \right] - y_0 \quad (2)$$

where

y_s is the live-bed average contraction scour depth, in ft;

y_1 is the average depth in the main channel of the approach section, in ft;

y_0 is the average depth in the contracted section before scour, in ft;

Q_1 is the discharge in the main channel of the approach section that is transporting sediment, in ft^3/s;

Q_2 is the discharge in the contracted section (bridge), in ft³/s;

W_1 is the width of the main channel of the approach section that is transporting sediment, in ft;

W_2 is the width (less pier widths) of the of the main channel in the contracted section (bridge) that is transporting sediment, in ft; and

k_1 is a coefficient determined by comparing shear velocity to the fall velocity of the D_{50} bed material (see Arneson and others, 2012, p. 6.10), which varies from 0.59 to 0.69.

Clear-Water Contraction Scour

If there is not continuous sediment transport between the approach section and contracted section, Arneson and others (2012) recommended using the clear-water contraction scour equation (eq. 3). The clear-water equation depends only on conditions in the contracted section and will calculate increasing scour for decreasing median sediment size. The clear-water equation will overestimate scour when the bridge section is narrow and deep, or when the bridge channel is armored with gravel significantly larger than the median. The clear-water equation does not consider the relative widths of the approach channel and bridge section, so no physical contraction is necessary to produce contraction scour.

$$y_s = \left[\frac{0.0077Q^2}{(1.25D_{50})^{2/3}W^2}\right]^{3/7} - y_0 \qquad (3)$$

where

y_s is the clear-water average contraction scour depth, in ft;

y_0 is the average depth in the contracted section before scour, in ft;

Q is the discharge in the contracted section, in ft³/s;

W is the width (less pier widths) of the of the main channel in the contracted section that is transporting sediment, in ft; and

D_{50} is the median diameter of bed material, in ft.

Vertical Contraction Scour

When flow is intercepted by the superstructure of a bridge and therefore no longer has a free surface, it undergoes vertical and horizontal contraction. These pressure flow conditions produce additional forces on the streambed and greater stress on the bridge (fig. 8). New bridges are designed with freeboard above the design scour floods to avoid vertical contraction, but some existing bridges are undersized relative to flooding that has occurred since they were designed and built. The 0.2-percent AEP flows produced vertical contraction conditions at 2 of the study sites. Vertical contraction scour without overtopping is calculated for live-bed and clear-water conditions using equations 4 and 5, respectively (Arneson and others, 2012; Shan and others, 2012). The equations are similar to those for horizontal contraction scour, but include a term comparing the depth of flow upstream of the bridge with the vertical opening of the bridge. The second term of both equations represents the estimated thickness of the separation zone, or zone of no flow, that forms under the downstream bridge superstructure (*T* in fig. 8). The separation zone further contracts the flow and increases scour.

$$y_s = \left[\left(\frac{Q_2}{Q_1}\right)^{6/7}\left(\frac{W_1}{W_2}\right)^{k_1} h_u\right] + \left[0.5\left(\frac{h_b(h_u - h_b)}{h_u^2}\right)^{0.2} h_b\right] - h_b \qquad (4)$$

where

y_s is the live-bed average vertical contraction scour depth, in ft;

Q_1 is the discharge in the main channel of the approach section that is transporting sediment, in ft³/s;

Q_2 is the discharge in the contracted section, in ft³/s;

W_1 is the width of the main channel of the approach section that is transporting sediment, in ft;

W_2 is the width (less pier widths) of the of the main channel in the contracted section that is transporting sediment, in ft;

h_u is the average depth in the upstream channel, in ft;

h_b is the vertical size of the bridge opening (low chord to average bed elevation) prior to scour, in ft; and

k_1 is a coefficient determined by comparing shear velocity to the fall velocity of the D_{50} bed material (see Arneson and others, 2012, p. 6.10), which varies from 0.59 to 0.69.

$$y_s = \left[\frac{0.0077Q_2^2}{(1.25D_{50})^{2/3}W_2^2}\right]^{3/7} + \left[0.5\left(\frac{h_b(h_u - h_b)}{h_u^2}\right)^{0.2} h_b\right] - h_b \qquad (5)$$

where

y_s is the clear-water average vertical contraction scour depth, in ft;

Q_2 is the discharge in the contracted section, in ft³/s;

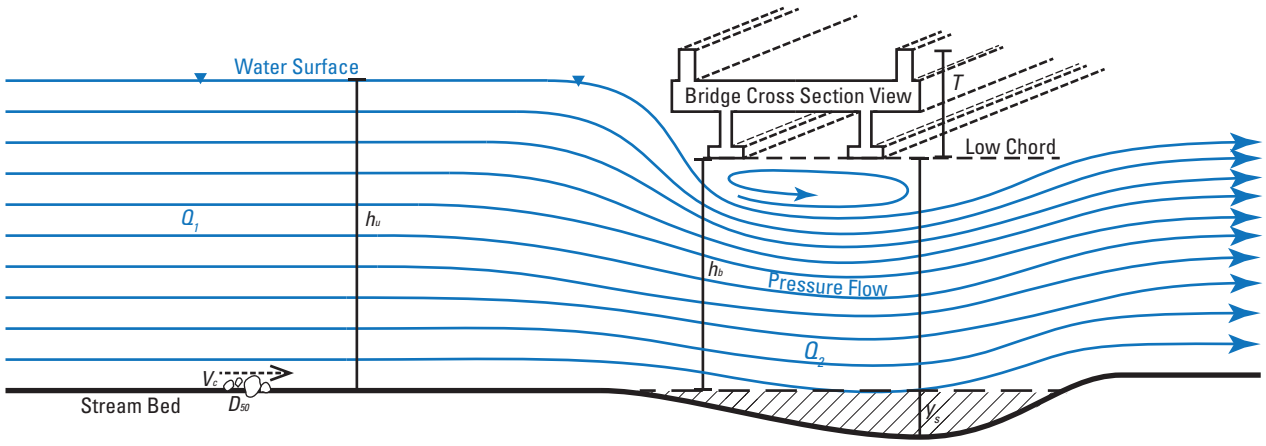

Figure 8. Example of vertical contraction scour and variables used to calculate scour. [Q_2, unit discharge at the approach cross section, in square feet per second; Q_1, unit discharge at the approach cross section, in square feet per second]

W_2 is the width (less pier widths) of the of the main channel in the contracted section, in ft;

D_{50} is the median diameter of bed material, in ft;

h_b is the vertical size of the bridge opening (low chord to average bed elevation) prior to scour, in ft; and

h_u is the average depth in the upstream channel, in ft.

Abutment Scour

The abutment scour method used in this study follows the National Highway Cooperative Research Program (NCHRP) Study 24-20 (Ettema and others, 2010) as recommended in HEC-18 (Arneson and others, 2012). The NCHRP 24-20 methods treat abutment scour as a local concentration of contraction scour, rather than an independent local scour component that is additive to contraction scour, like pier scour. The contraction creates flow separation vortices adjacent to abutments when they encroach on the active flow area (fig. 9; Ettema and others, 2010). The NCHRP 24-20 study also concluded that abutment scour is limited by the geotechnical stability of the embankments, which fail and fill in scour holes when they are undercut. Riprap cover (when present) travels downslope and concentrates flow and the deepest scour on the downstream corner of the abutment (Ettema and others, 2010). Minor embankment failures and erosion were noted at 11 of study sites according to ADOT&PF inspection report. Presence of adequate riprap was extracted from DOT inspection reports and is noted in the results.

All sites in this study resemble condition A, defined in NCHRP 24-20, as where the abutment is located at or near the main channel. At Willow Creek Bridge 1831, the right abutment has already lost all approach fill and is treated like a pier. Equation 6 includes an estimate of contraction scour and an amplification factor related to the relative concentration of flow under the bridge for condition A. Arneson and others (2012) suggested using a live-bed equation to calculate contraction scour for condition A, but critical velocity computations show that clear-water contraction scour occurred at many sites. Equation 6 was used with the contraction scour value calculated separately, whether live-bed, clear-water, or vertical contraction equations were used. The amplification factor is determined using figure 10, which consists of empirically derived curves relating relative contraction (q_2/q_1) as calculated in equation 7 to α_A for spill-through and wingwall type abutments. The amplification factor peaks for wingwall and spill-through abutments at just under 1.8 and 1.7 when relative contraction is about 1.3 and 1.2, respectively (fig. 6). The physical reason for this is that flow separation dominates the abutment scour process at moderate contraction ratios, whereas contraction scour dominates at higher contraction ratios. Thus, equation 6 will produce large abutment scour estimates for sites with modest contraction and deep channels, even if contraction scour is small.

$$y_s = \left(\alpha_A y_c\right) - y_0 \tag{6}$$

where

y_s is the abutment scour depth, in ft;

α_A is the amplification factor for live-bed conditions (fig. 8);

y_c is the average flow depth at the bridge including contraction scour, in ft; and

y_0 is the flow depth at the bridge prior to scour, in ft.

$$\frac{q_2}{q_1} = \frac{Q_1/W_1}{Q_2/W_2} \tag{7}$$

where

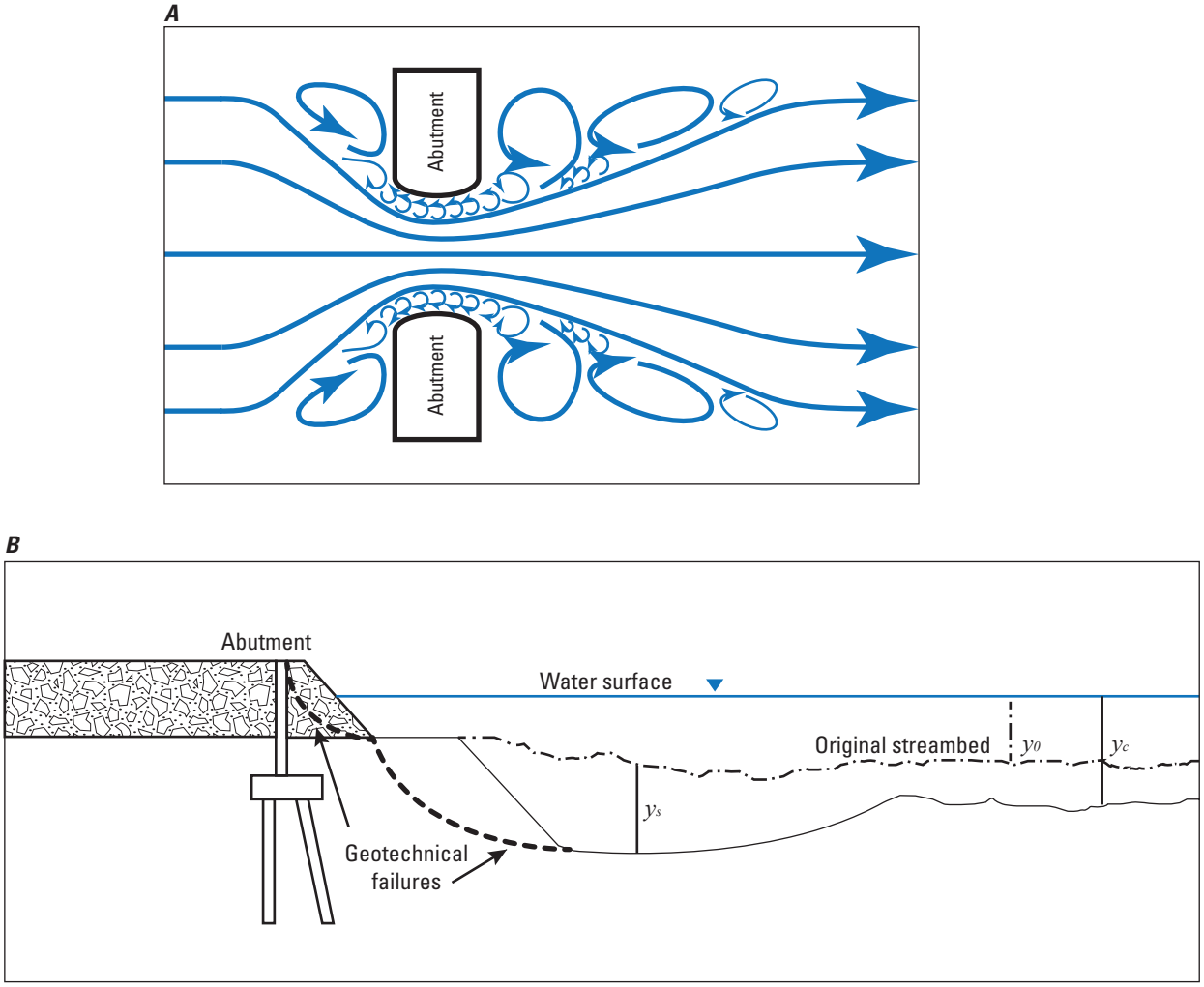

Figure 9. Examples of abutment scour plan (*A*) and cross-section (*B*) views. [Modified from Ettema and others (2010). Variables are defined in equation 6]

q_2 is the unit discharge at the bridge, in square foot per second (ft^2/s);

q_1 is the unit discharge at the approach cross section, in ft^2/s;

Q_1 is the discharge at the bridge, inft^3/s;

Q_2 is the discharge at the approach section, in ft^3/s;

W_1 is the flow top width at the bridge, in ft; and

W_2 is the flow top width at the approach section, in ft.

Pier Scour

The undermining of bridge piers from scour is a major cause of bridge failure. During floods, piers obstruct flow and cause water to pile up at the upstream end of the pier (fig. 11). This creates horseshoe-shaped vortices that plunge downward around the nose of the pier, scouring bed material from around the base. Scour continues until it reaches an equilibrium depth where the vortices are no longer strong enough to move bed material, similar to contraction scour. Arneson and others (2012) recommended use of equation 8 for most conditions. However, Shan and others (2016) recommends modifying and expanding the use of the coarse-bed pier scour equation to a wider range of conditions. The Hager number/gradation coefficient (HN/GC) equation, equation 9, is similar in form to equation 8, but includes terms that account for bed material size and gradation. Both equations were used for comparison. Tables for each of the correction factors K_1 to K_3 are in Arneson and others (2012, chap. 7). Pier scour depends on flow depth immediately upstream of the pier, velocity at the pier, and the width of the pier, and on grain size. Neither site required a flow angle correction factor. An upper bound for scour depths at cylindrical or round-nosed piers aligned to flow is 2.4 times the pier width for Froude numbers less than 0.8 (Arneson and others, 2012). This applies to Ward Creek Bridge 747 and the abutment piles at Willow Creek 1831. The

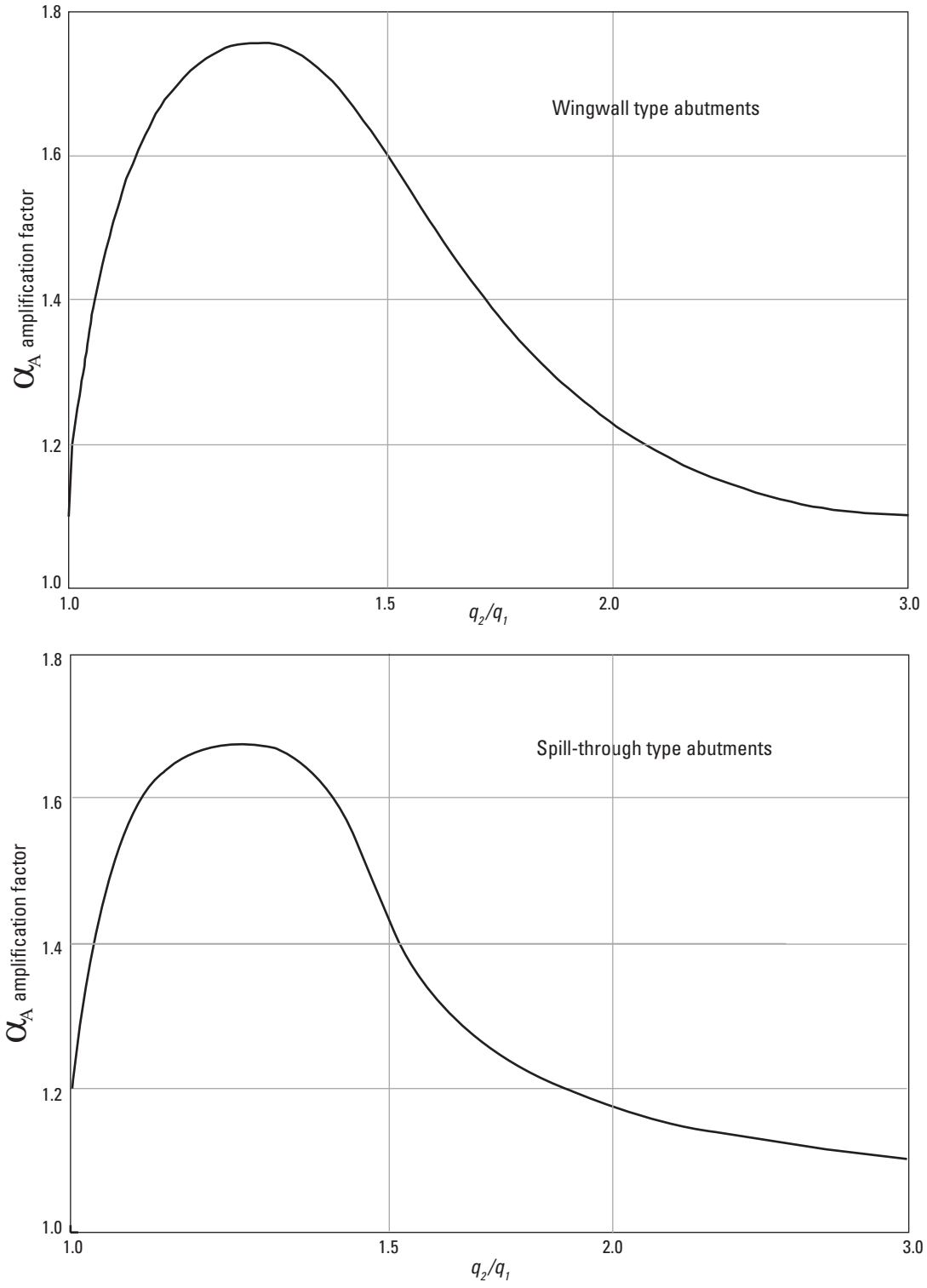

Figure 10. Amplification factor for live-bed abutment scour (q_2/q_1, relative contraction) for wingwall (*A*) and spill-through type abutments (*B*). [Figure is modified from Ettema and others (2010). α_A, is the amplification factor for live-bed conditions]

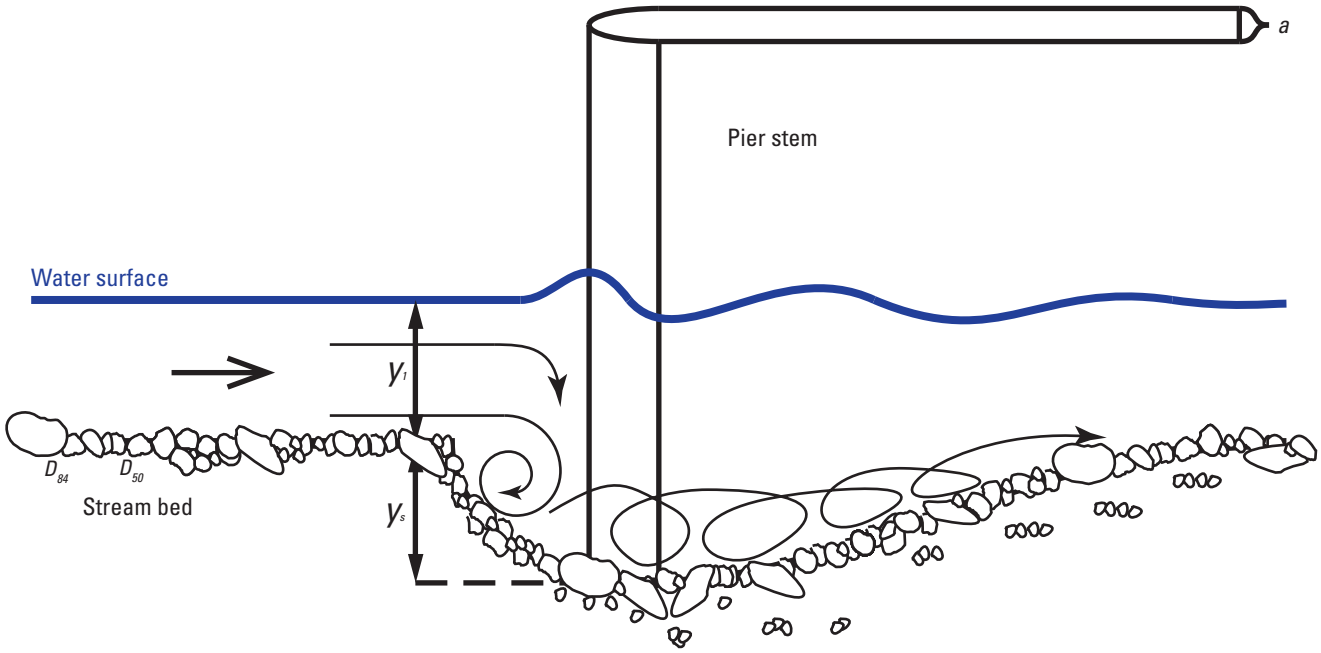

Figure 11. Example of pier scour with variables used to calculate scour. [y_1, is the flow depth directly upstream of the pier (in feet); y_s, is the pier scour depth (in feet)].

piers at Willow Creek are unusual in that they are composed of unevenly spaced piles of different diameters under rectangular sheet pile walls that extend to the streambed or slightly above. These are represented in the model and equations as simple rectangular piers. This may produce conservative results when the streambed scours below the sheet pile walls, but removes the uncertainty caused by the uneven diameters and spacing of the piles.

Variables for pier scour were extracted from the two-dimensional models in two ways. The first estimate is the "maximum pier scour" for the bridge, in which all the elements of the mesh for about 10 ft upstream of the bridge face are selected and the maximum Froude number (velocity times depth) values are extracted. This is how pier scour is routinely calculated with one-dimensional models (Arneson and others, 2012). The next estimate is specific to each pier, where the maximum depth and velocity are extracted from the mesh just upstream of the pier of interest. The abutment piles on the right bank of Bridge 1831 are considered piers for this study because they are now mid-flow in the river following failure of the embankment.

$$y_s = 2y_1K_1K_2K_3\left(\frac{a}{y_1}\right)^{0.65}\left(\frac{V_1}{\sqrt{gy_1}}\right)^{0.43} \quad (8)$$

where

y_s is the pier scour depth, in ft;

K_1 is the correction factor for pier nose shape 1 for round piers (1.1 for rectangular piers);

K_2 is the correction factor for angle of attack of flow;

K_3 is the correction factor for bed condition, assumed to be 1.1 for the small streams in this study;

y_1 is the flow depth directly upstream of the pier, in ft;

a is the pier width, in ft;

V_1 is the mean velocity directly upstream of the pier, in foot per second; and

g is the acceleration of gravity, 32.2 feet per square second.

$$y_s = 1.32K_1K_2K_3a^{0.62}y_1^{0.38}tanh\left(\frac{H^2}{1.97\sigma^{1.5}}\right) \quad (9)$$

$$H = \left(\frac{V_1}{\sqrt{g\left(S_g - 1\right)D_{50}}}\right) \quad (9.1)$$

$$\sigma = \frac{D_{84}}{D_{50}} \quad (9.2)$$

where

H is the densimetric particle Froude number (eq. 9.1);
S_g is the sediment specific gravity (assumed to be 2.65)
;σ is the sediment gradation coefficient (eq. 9.2); and
D_{84} is the grain diameter of which 84 percent are smaller, in ft.

Clear-water and live-bed scour estimates for sites with horizontal contraction scour at the design and (or) check floods where the water surface did not reach the low chord of the bridge are shown in table 7. These estimates range from no scour to 5.1 ft and indicate mostly clear-water conditions, although both estimates are shown for each site. At Wasilla Creek 2227, modeled velocities indicated continuous live-bed transport through the reach. However, live-bed scour was much higher than clear-water scour, indicating that armoring would likely limit scour to the clear-water estimate (Arneson and others, 2012). Vertical contraction was minor, with the 0.2-percent AEP flow reaching 0.7 ft above the low chord at Little Susitna Bridge 2225 (table 8). Abutment scour, which is treated as an amplification of contraction scour, ranges from 0 to 5.9 ft (table 9).

Pier scour is listed in table 10 for each pier at Ward Creek Bridge 747 and Willow Creek Bridge 1831. Pier scour ranged from 2 to 5.8 ft using local velocity and depth upstream of each pier, and from 5.2 to 7 ft using the maximum depth/velocity product in the section upstream of the bridge. The maximum depth/velocity product is used to illustrate what might happen should the highest energy part of the channel migrate to the pier. For comparison, the HEC-18 equation 1 are also shown. These are consistently higher, primarily because the HEC-18 equation does not consider the coarse bed materials. Contraction scour adds 0–1.4 ft to the pier scour.

Bridges with High Scour Estimates

The threshold for "substantial scour" was considered 5 ft in some previous Alaskan studies (Beebee and Schauer, 2015; Beebee and others, 2017), while 4 ft was the threshold in Conaway and Schauer (2012). These numbers are somewhat arbitrary, and the influence of scour on the bridge structure ultimately depends on the depth of the bridge foundations. Those bridges coded as U in table 1 are founded on piles of unknown depth; thus, these numbers may be used to prioritize bridge for pile-depth testing. Pier scour of 5 ft or more is estimated for Willow Creek 1831 (coded U) and Ward Creek 747. Abutment scour estimates at Wasilla Creek 2227 and Ship Creek 1940 were greater than 5 ft and at Ward Creek 747 were greater than 4 ft. Willow Creek 1831 is already closed after abutment and approach fill loss during the 2012 flood. Wasilla Creek 2227 has a fine-grained bed and field observations indicated scour holes several feet deep at bends upstream and downstream of the bridge. Ship Creek 1940 has a relatively fine-grained bed and vertical sheet-pile abutments encroaching on the main channel.

Because most of the bridges in this study cross small streams with coarse gravel beds, the concentrated flow through the bridge is not energetic enough to produce high scour estimates even though there is often substantial contraction in width at the bridge. An additional factor that reduces scour estimates is pre-existing scour. All estimates use the contracted cross-section measured after a bridge had been in place for many years. The contracted section may have been scoured to equilibrium depth several times, and on streams with low sediment transport, this scour hole would be slow to fill in. A third scour-reducing factor that is more easily recognized in two-dimensional models than in one-dimensional models is overflow of road approaches. At 11 study sites, low road approaches on floodplains convey as much 35 percent of the 1-percent AEP flow, relieving contraction.

Comparisons of Results for Bridges with Both One-Dimensional and Two-Dimensional Models

Little Susitna River Braid Bridge 1713

Bridge 1713, built in 2011, spans a sub-channel of the Little Susitna River in a braided reach. An indefinite proportion of the estimated 1- and 0.2-percent AEP flows would enter this channel so, for the one-dimensional model, a "maximum pressure flow" was determined that would fill the channel to capacity without losing substantial flow to the road approach. This flow is 5,450 ft^3/s, compared to estimates of 8,970 and 12,100 ft^3/s for the 1- and 0.2-percent AEP flows (Beebee and others, 2017). Estimated vertical contraction and abutment scour were 5.8 and 13.1 ft, respectively. The two-dimensional model was used both to distribute flow between sub-channels of the Little Susitna River and derive hydraulic variables used to calculate scour. The model computed that 1,570 and 1,847 ft^3/s would flow through the 1713 bridge at the 1- and 0.2-percent AEP flows, respectively. Neither flood reached the low chord of the bridge. Most of the flood flow was conveyed across the floodplain and over low road approaches. Estimated contraction and abutment scour for Bridge 1713 using the two-dimensional model were 0.3 and 1.3 ft, respectively, only 10 percent of the earlier estimate.

Table 7. Hydraulic variable estimates of horizontal contraction scour for selected bridge sites in Alaska with no pressure flow.

[D_{50}: Median grain diameter. **Abbreviations**: AEP, annual exceedance probability; ft, foot; ft/s, foot per second; ft^3/s, cubic foot per second; %, percent]

Bridge No.	River or stream	Event	Width of approach channel (ft)	Discharge at approach channel (ft^3/s)	Flow depth in approach (ft)	Width of channel at bridge (ft)	Discharge at bridge channel (ft^3/s)	Depth of flow at bridge (ft)	D_{50} (ft)	Critical velocity for D_{50} (ft/s)
1712	Cottonwood Creek	1% AEP flood	37.9	83	0.8	13.0	75	1.3	0.11	5.1
		.2% AEP flood	37.9	128	1.1	13.0	97	1.6	0.11	5.4
2207	Cottonwood Creek	1% AEP flood	19.1	477	5.7	22.0	632	5.9	0.14	7.7
		.2% AEP flood	19.1	542	5.8	22.0	793	6.5	0.14	7.7
1709	Little Susitna River at Moose Meadows	1% AEP flood	25.8	945	6.6	22.8	1,368	7.4	0.13	7.8
		.2% AEP flood	25.2	988	6.9	22.8	1,496	7.7	0.13	7.8
2225	Little Susitna River at Reed[1]	1% AEP flood	50.7	1,379	4.4	45.1	1,577	6.8	0.17	7.9
		.2% AEP flood	50.7	1,525	4.8	45.1	1,580	7.3	0.17	8.0
1713	Little Susitna River at Welch	1% AEP flood	37.7	1,253	5.6	21.0	946	5.1	0.13	7.5
		.2% AEP flood	37.7	1,423	6.2	21.1	1,106	5.6	0.13	v7.7
811	Livengood Creek	1% AEP flood	14.1	559	4.7	15.8	621	4.8	0.11	6.9
		.2% AEP flood	23.8	950	5.3	21.1	987	5.6	0.11	7.1
1985	Moose Creek	1% AEP flood	34.2	834	9.2	48.6	2,595	8.3	0.10	7.5
		.2% AEP flood	34.2	848	9.8	53.1	2,843	8.8	0.10	7.6
1018	North Fork Anchor River	1% AEP flood	41.6	1,188	4.7	20.9	1,205	7.2	0.10	6.7
		.2% AEP flood	41.6	1,231	5.5	20.9	1,539	7.9	0.10	6.9
812	Peters Creek	1% AEP flood	154.6	4,307	6.5	122.7	5,562	8.8	0.10	7.1
		.2% AEP flood	154.6	5,052	7.9	123.7	6,814	9.4	0.10	7.3
2226	Sawyer Creek	1% AEP flood	15.9	571	5.5	23.1	1,057	5.0	0.10	6.9
		.2% AEP flood	15.9	669	6.1	23.1	1,209	5.4	0.10	7.0
1199	South Fork Anchor River	1% AEP flood	66.7	2,292	6.5	51.6	3,154	6.8	0.14	8.0
		.2% AEP flood	66.7	2,493	6.9	51.6	3,451	7.1	0.14	8.1
1940	Ship Creek	1% AEP flood	61.3	2,614	5.0	98.1	4,459	5.2	0.11	7.0
		.2% AEP flood	80.0	4,100	5.8	100.2	5,779	6.0	0.11	7.2
2206	Twin Creek	1% AEP flood	25.3	575	4.4	24.6	651	3.7	0.09	6.5
		.2% AEP flood	25.3	697	5.0	24.6	802	4.0	0.09	6.6
747	Ward Creek	1% AEP flood	116.7	4,486	8.0	42.8	3,784	11.8	0.06	6.1
		.2% AEP flood	116.7	5,625	9.2	48.4	5,140	12.9	0.06	6.3
1708	Wasilla Creek	1% AEP flood	17.1	301	3.7	19.4	349	3.1	0.15	7.4
		.2% AEP flood	17.1	341	4.2	19.4	452	3.6	0.15	7.6
2227	Wasilla Creek[2]	1% AEP flood	13.7	143	5.2	29.3	441	3.6	0.00	1.9
		.2% AEP flood	13.7	135	5.7	29.3	593	4.0	0.00	1.9
2238	Wasilla Creek	1% AEP flood	15.9	127	3.6	24.0	396	2.9	0.15	7.4
		.2% AEP flood	15.9	185	4.6	24.0	537	3.4	0.15	7.7
2286	Wasilla Creek	1% AEP flood	17.6	282	4.0	27.7	388	3.8	0.15	7.5
		.2% AEP flood	18.5	348	4.2	27.8	535	4.1	0.15	7.5
1782	Willow Creek	1% AEP flood	195.8	9807	6.6	103.0	8380	7.5	0.21	9.1
		.2% AEP flood	195.8	11,836	7.6	105.1	10,053	8.1	0.21	9.3
		1987 flood	195.9	9,639	6.5	103.0	8,251	7.4	0.21	9.1
1831	Willow Creek	1% AEP flood	69.5	4,301	5.8	55.1	5,743	9.2	0.27	9.7
		.2% AEP flood	98.4	8,082	6.6	81.9	9,068	9.5	0.27	9.9
		1987 flood	69.5	4,223	5.7	55.1	5,650	9.1	0.27	9.7

Table 7. Hydraulic variable estimates of horizontal contraction scour for selected bridge sites in Alaska with no pressure flow.—Continued

Bridge No.	Modeled velocity in the approach channel (ft/s)	Likely type of scour	Depth of live-bed contraction scour (ft)	Depth of clear-water contraction scour (ft)
1712	2.7	Clear	0.1	0.0
	3.0	Clear	0.1	0.0
2207	4.9	Clear	0.7	0.0
	4.9	Clear	0.9	0.0
1709	5.5	Clear	2.4	0.0
	5.7	Clear	2.9	0.0
2225	6.2	Clear	0.0	0.0
	6.2	Clear	0.0	0.0
1713	6.0	Clear	1.2	0.3
	6.1	Clear	1.6	0.6
811	7.6	Live	0.0	0.3
	8.5	Live	0.3	0.3
1985	2.7	Clear	11.1	0.0
	2.5	Clear	12.2	0.0
1018	6.1	Clear	0.2	0.1
	5.4	Clear	2.5	1.0
812	4.3	Clear	0.6	0.0
	4.5	Clear	2.4	0.0
2226	6.5	Clear	2.4	0.9
	7.0	Clear	2.5	1.3
1199	5.3	Clear	3.3	0.1
	5.4	Clear	3.7	0.4
1940	8.6	Live	0.6	0.0
	8.8	Live	0.8	1.1
2206	5.2	Clear	1.3	0.2
	6.1	Clear	1.8	0.6
747	4.8	Clear	1.3	0.4
	5.3	Clear	2.1	1.4
1708	4.7	Clear	0.8	0.0
	4.8	Clear	1.3	0.0
2227	2.2	Live	8.4	3.1
	1.9	Live	12.5	5.1
2238	2.2	Clear	4.4	0.0
	2.7	Clear	5.4	0.0
2286	4.1	Clear	3.8	0.0
	4.5	Clear	4.5	0.0
1782	7.6	Clear	1.3	0.4
	8.0	Clear	1.7	1.0
	7.5	Clear	1.2	0.4
1831	10.7	Clear	0.0	0.0
	12.5	Clear	0.0	0.1
	10.6	Clear	0.0	0.0

[1]Vertical contraction occurs here. See Table 8.

[2] Because live-bed scour is greater than clear-water scour, armoring will probably limit scour to the clear-water estimate.

Table 8. Hydraulic variables and estimates of vertical contraction scour for Bridge 2225, Little Susitna at Reed, Alaska.

[**Abbreviations**: ft, foot; ft/s, foot per second; ft^3/s, cubic foot per second]

Bridge No.	River or stream	Event	Top of bridge superstructure elevation (ft)	Low chord elevation (ft)	Water surface elevation, upstream side of bridge (ft)	Weir flow	Depth at upstream side of bridge (h_u) (ft)	Bridge opening height (h_b) (ft)	Discharge through bridge (Q_2) (ft^3/s)	Discharge through approach channel (Q_1) (ft^3/s)	Width of approach channel (W_1) (ft)	Width of bridge opening (W_2) (ft)
2225	Little Susitna at Reed	1% AEP flood	561.0	558.1	558.3	No	4.2	4	1,655	1,628	128.8	66.8
		.2% AEP flood	561.0	558.1	558.8	No	4.7	4	1,821	1,942	128.8	66.8

Bridge No.	Depth at approach channel (ft)	Live-bed coefficient (K_1)	Critical velocity (ft/sec)	Velocity at the approach (ft/sec)	Vertical contraction scour depth live-bed (ft)	Vertical contraction scour depth clear-water (ft)	Indicated type of scour
2225	2.5	0.6	7.2	3.8	3.4	0.0	Clear
	2.8	0.6	7.3	3.9	3.8	0.5	Clear

Table 9. Estimated abutment scour and variables for selected bridge sites in Alaska.

[**Abutment type**: ST, spill through; WW, wingwall. **Abbreviations**: AEP, annual exceedance probability; Max, maximum; ft, foot; ft^2/s square foot per second; ft^3/s, cubic foot per second]

Bridge No.	River or stream	Event	Adequate riprap	Abutment type	Total approach width (ft)	Total approach discharge (ft^3/sec)	Total bridge opening width (ft)	Total discharge at bridge (ft^3/sec)	Contraction scour (ft)	Hydraulic depth at bridge (ft)	Live bed amplification factor α	Flow depth at bridge including contraction and abutment scour (ft)	Maximum scour depth at abutment (ft)
1712	Cottonwood Creek	1% AEP flood	N	ST	45.5	84	22.1	76	0.0	0.9	1.2	1.1	0.2
		.2% AEP flood			45.7	132	22.7	120	0.0	1.1	1.2	1.4	0.2
2207	Cottonwood Creek	1% AEP flood	N	ST	161.4	671	45.4	706	0.0	3.8	1.1	4.2	0.4
		.2% AEP flood			184.3	894	46.3	932	0.0	4.3	1.1	4.7	0.4
1709	Little Susitna River at Moose Meadows	1% AEP flood	Y	ST	316.4	1,987	58.6	1,929	0.0	4.5	1.1	4.9	0.4
		.2% AEP flood			322.2	2,315	58.5	2,160	0.0	4.8	1.1	5.2	0.5
2225	Little Susitna River at Reed	1% AEP flood	Y	ST	128.9	1,625	72.5	1,609	0.0	5.0	1.2	6.1	1.1
		.2% AEP flood			137.3	1,848	72.5	1,611	0.5	5.5	1.3	7.8	2.3
1713	Little Susitna River at Welch	1% AEP flood	Y	ST	120.5	1,452	51.7	1,570	0.3	4.2	1.2	5.4	1.3
		.2% AEP flood			180.9	1,716	54.6	1,847	0.6	4.5	1.1	5.5	1.1
811	Livengood Creek	1% AEP flood	N	WW	27.8	732	21.1	698.8	0.0	4.1	1.3	5.9	1.6
		.2% AEP flood			39.2	1,002	21.1	1,040.8	0.3	4.3	1.6	9.0	3.8
1985	Moose Creek	1% AEP flood	Y	WW	683.1	2,961	57.9	2,756	0.0	7.7	1.1	8.5	0.8
		.2% AEP flood			686.1	3,551	57.9	2,952	0.0	8.5	1.1	9.4	0.9
1018	North Fork Anchor River	1% AEP flood	Y	WW	350.7	1,796	38.7	1,842	0.1	10.1	1.1	11.3	1.1
		.2% AEP flood			415.2	2,399	38.7	2,439	1.1	11.2	1.1	13.5	2.3
812	Peters Creek	1% AEP flood	Y	ST	802.5	5,918	151.3	5,658	0.0	7.5	1.1	8.2	0.7
		.2% AEP flood			802.5	7,553	151.3	6,921	0.0	8.1	1.1	8.9	0.8
2226	Sawyer Creek	1% AEP flood	Y	ST	96.0	1,268	32.4	1,156	0.9	4.1	1.1	5.6	1.5
		.2% AEP flood			96.0	1,647	32.4	1,329	1.3	4.4	1.1	6.5	2.1

Table 9. Estimated abutment scour and variables for selected bridge sites in Alaska.—Continued

Bridge No.	River or stream	Event	Adequate riprap	Abutment type	Total approach width (ft)	Total approach discharge (ft^3/sec)	Total bridge opening width (ft)	Total discharge at bridge (ft^3/sec)	Contraction scour (ft)	Hydraulic depth at bridge (ft)	Live bed amplification factor α	Flow depth at bridge including contraction and abutment scour (ft)	Maximum scour depth at abutment (ft)
1199	South Fork Anchor River	1% AEP flood	N	WW	832.9	5,201	68.1	3,898	0.1	6.7	1.1	7.5	0.8
		.2% AEP flood			840.7	6,713	68.1	4,269	0.4	7.0	1.1	8.1	1.1
1940	Ship Creek	1% AEP flood	N	WW	154.3	4,685	113.9	4,591	0.6	5.2	1.8	10.2	5.0
		.2% AEP flood			159.2	6,046	113.9	5,906	0.8	5.5	1.7	10.7	5.2
2206	Twin Creek	1% AEP flood	N	ST	142.0	721	34.9	715	0.2	2.9	1.1	3.4	0.5
		.2% AEP flood			182.0	970	34.9	888	0.6	3.3	1.1	4.2	0.9
747	Ward Creek	1% AEP flood	Y	ST	158.5	4,614	88.1	4,613	0.4	8.5	1.2	10.8	2.4
		.2% AEP flood			160.4	5,734	91.3	5,727	1.4	8.8	1.2	12.5	3.7
1708	Wasilla Creek	1% AEP flood	Y	WW	207.9	403	45.5	427	0.0	1.9	1.1	2.1	0.2
		.2% AEP flood			221.1	581	42.5	592	0.0	1.0	1.0	1.0	0.0
2227	Wasilla Creek	1% AEP flood	N	ST	347.4	471	39.0	449	3.1	2.9	1.1	6.6	3.7
		.2% AEP flood			355.1	651	39.0	611	5.1	3.3	1.1	9.2	5.9
2238	Wasilla Creek	1% AEP flood	N	ST	310.0	453	33.5	432	0.0	2.4	1.1	2.6	0.2
		.2% AEP flood			314.5	632	36.3	598	0.0	2.5	1.1	2.8	0.3
2286	Wasilla Creek	1% AEP flood	Y	ST	138.2	397	37.8	393	0.0	3.0	1.1	3.3	0.3
		.2% AEP flood			195.6	567	37.8	546	0.0	3.4	1.1	3.7	0.3
1782	Willow Creek	1% AEP flood	Y	WW	272.2	10,576	128.5	8,882	0.4	7.2	1.3	10.1	2.9
		.2% AEP flood			295.7	13,299	128.5	10,494	1.0	7.8	1.3	11.7	3.9
		1987 flood			282.3	10,398	128.5	8746	0.4	7.2	1.3	10.0	2.9
1831	Willow Creek	1% AEP flood	N	WW	556.9	12,246	222.9	11,721	0.0	6.2	1.1	7.0	0.8
		.2% AEP flood			562.2	16,662	222.9	15,607	0.1	7.3	1.1	8.3	1.0
		1987 flood			556.9	12,001	222.9	11,490	0.0	6.1	1.1	6.9	0.8

Table 10. Hydraulic variables and estimated pier scour at two bridge sites in Alaska with piers.

[D_{50}: Median grain diameter. D_{84}: 84th percentile grain diameter. K_1: pier nose shape coefficient; K_2: flow angle coefficient. **Abbreviations**: AEP, annual exceedance probability; ft, foot; ft/s foot per second]

Bridge No.	River or stream	Events	Velocity upstream of pier (ft/s)	Depth upstream of pier (ft)	Pier Nose Shape K_1	K_2	Pier Width (ft) a	D_{50}	D_{84}	Shen (2016) pier scour estimate (ft)	HEC-18 pier scour estimate (ft)	Contraction scour (ft)	Total scour at pier (ft)
747	Ward Creek Pier 1	1% AEP flood	3.3	8.4	1.0	1.2	1.17	0.10	0.17	2.0	3.4	0.4	2.4
	Pier 2	1% AEP flood	5.1	5.5	1.0	1.0	1.17	0.10	0.17	2.5	3.2	0.4	2.9
	Pier 1	.2% AEP flood	3.8	8.9	1.0	1.2	1.17	0.10	0.17	2.5	3.6	1.4	3.9
	Pier 2	.2% AEP flood	5.6	6.7	1.0	1.0	1.17	0.10	0.17	2.9	3.4	1.4	4.3
747	Ward Creek Maximum Depth/Velocity Product	1% AEP flood	7.4	11.5	1.0	1.2	1.17	0.10	0.17	4.8	5.0	0.4	5.2
		.2% AEP flood	8.2	13.4	1.0	1.2	1.17	0.10	0.17	5.1	5.3	1.4	6.5
	Willow Pier 1	1% AEP flood	5.8	5.1	1.1	1.0	2.83	0.27	0.51	2.5	6.5	0.0	2.5
	Pier 2	1% AEP flood	8.0	5.4	1.1	1.0	2.25	0.27	0.51	3.6	6.1	0.0	3.6
	Pier 3	1% AEP flood	8.8	6.4	1.1	1.0	2.83	0.27	0.51	4.9	7.2	0.0	4.9
	Pier 4	1% AEP flood	9.3	11.8	1.0	1.0	0.83	0.27	0.51	2.8	3.6	0.0	2.8
	Willow Pier 1	.2% AEP flood	6.9	6.4	1.1	1.0	2.83	0.27	0.51	3.6	6.5	0.1	3.7
	Pier 2	.2% AEP flood	8.9	6.8	1.1	1.0	2.25	0.27	0.51	4.4	6.3	0.1	4.5
	Pier 3	.2% AEP flood	9.8	7.8	1.1	1.0	2.83	0.27	0.51	5.8	7.7	0.1	5.9
	Pier 4	.2% AEP flood	9.7	13.3	1.0	1.0	0.83	0.27	0.51	3.0	3.5	0.1	3.1
	Willow Pier 1	1987 flood	5.7	5.0	1.1	1.0	2.83	0.27	0.51	2.4	5.9	0.0	2.4
	Pier 2	1987 flood	7.9	5.3	1.1	1.0	2.25	0.27	0.51	3.5	6.0	0.0	3.5
	Pier 3	1987 flood	8.7	6.3	1.1	1.0	2.83	0.27	0.51	4.8	7.0	0.0	4.8
	Pier 4	1987 flood	9.3	11.7	1.0	1.0	0.83	0.27	0.51	2.7	3.5	0.0	2.7
1831	Willow Creek Maximum Depth/Velocity Product	1% AEP flood	9.3	11.8	1.1	1.0	2.83	0.27	0.51	6.5	6.9	0.0	6.5
		.2% AEP flood	9.7	13.3	1.1	1.0	2.83	0.27	0.51	7.0	7.4	0.1	7.1
		1987 flood	9.3	11.7	1.1	1.0	2.83	0.27	0.51	6.5	6.9	0.0	6.5

North Fork Anchor River Bridge 1018

Estimated abutment scour at North Fork Anchor 1018 using the one-dimensional model was 4.7–6.3 ft for the 1- and 0.2-percent AEP flows, respectively. A 5-ft-deep scour hole was noted in a 2005 inspection at the right abutment toe, and inspection reports consistently note failure of the embankments and gabions placed to protect the abutments. A 90-degree bend in the channel approaching the bridge exposes the right abutment to increased hydraulic forces and flow separation that are unaccounted for in the one-dimensional model.

Extensive bank stabilization efforts in 2015 armored the banks, improved the approach angle, and increased channel capacity. The two-dimensional model including bank improvements shows 1.1 to 2.3 ft of abutment scour at the 1- and 0.2-percent AEP flows, respectively. The one-dimensional and two-dimensional models can't really be compared because of the changes in channel geometry.

South Fork Anchor River Bridge 1199

The one-dimensional model showed that the 0.2-percent AEP flow at South Fork Anchor River reaches the superstructure of the bridge and creates vertical contraction scour of 5.9 ft and abutment scour of 7.3 ft. The two-dimensional model showed that the 0.2-percent AEP flow reached to 0.2 ft below the low chord of the bridge, narrowly avoiding pressure flow, and resulted in 1.1 ft of abutment scour. The two-dimensional model routed about 35 percent of the 0.2-percent AEP flow over the road approach, providing significant relief to the structure. Although use of the two-dimensional model reduced scour estimates, it illustrates other potential problems with the bridge. Both main channel and floodplain flow enters the bridge at a nearly 45-degree angle causing flow separation at the downstream left bank abutment, an area where DOT inspection notes indicate riprap loss and erosion. Hydraulic parameters in the two-dimensional model were used to delineate an area of clear water scour potential at the 0.2-percent AEP flow near this abutment (fig. 12).

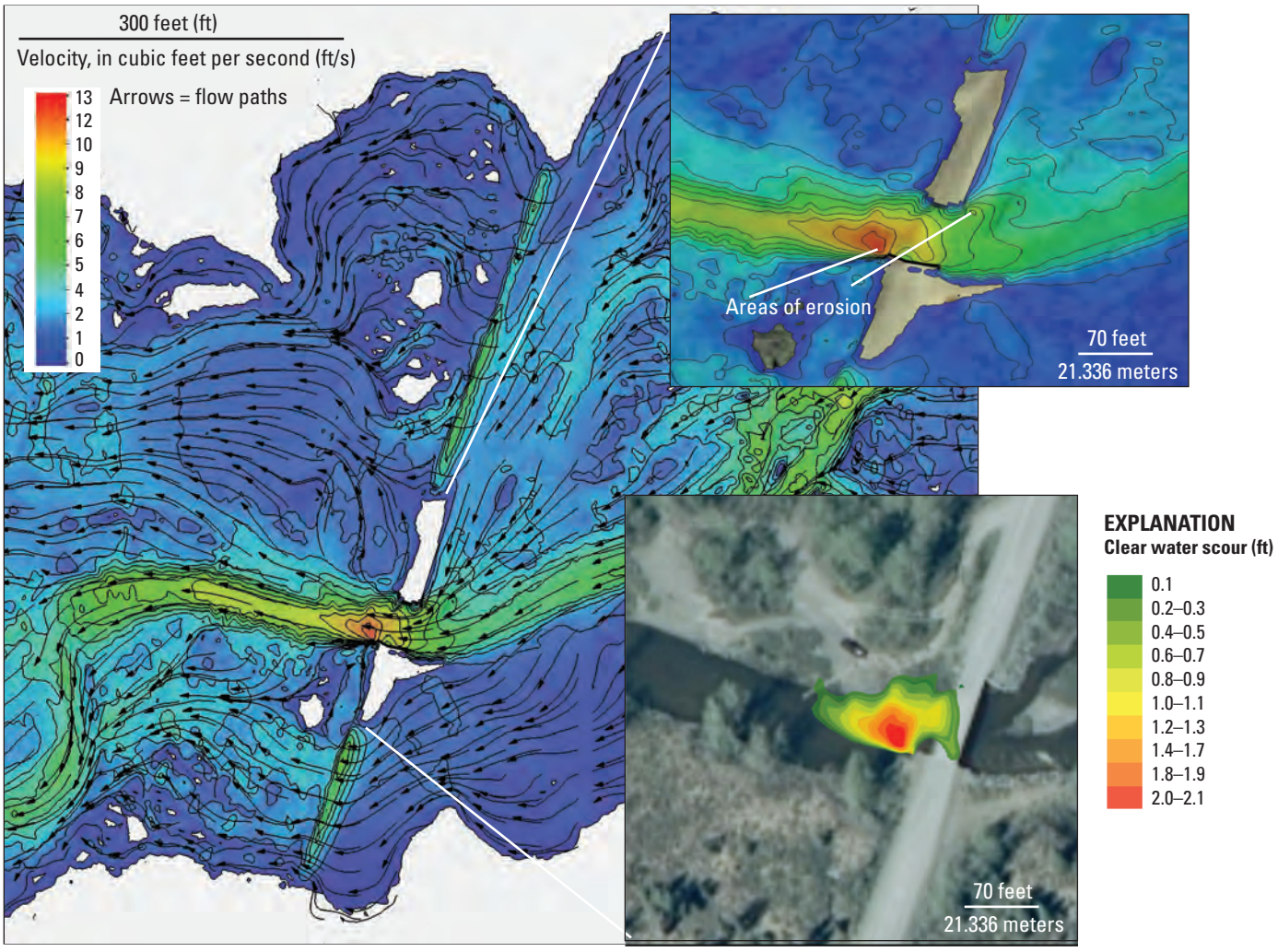

Figure 12. Flow patterns and calculated clear-water scour from a two-dimensional simulation of the 0.2-percent annual exceedance probability flow at South Fork Anchor River Bridge 1199, Alaska.

Summary and Conclusions

Twenty bridge sites in Alaska were evaluated for streambed scour, including reach-scale stream stability, contraction scour, and local scour at piers and abutments. Most channels were classified as stable, but two channels were classified as less stable or unstable: one likely related to mining, and one likely related to changing flow distribution. Scour estimates are less reliable for unstable sites because the equations assume static channel geometry. Changing flow distribution adds even more uncertainty.

Design and check floods were determined for 20 sites and all were modeled with SRH-2D. The design and check floods used to calculate scour for most bridges were the estimated 1-percent and 0.2-percent AEP flows, respectively, but for distributary sites where standard flood frequency techniques weren't applicable, SRH-2D was used to distribute the calculated design and check floods between channels. Scour was calculated for large observed floods at two sites.

Contraction scour and abutment scour were calculated for all 20 bridges, and pier scour was calculated for the 2 bridges with piers. Vertical contraction occurred during the design and check floods at one site. Overflow on road approaches reduced flood flow under bridges and thus contraction and abutment scour.

Use of the coarse-bed pier equation, which considers the grain-size distribution in the channel, decreased estimated scour compared to the simple pier scour equation. At Ward Creek, the decrease was 4–43 percent, and at the coarser-bedded Willow Creek 1831, the decrease was 25–64 percent.

The use of two-dimensional models improves scour estimates by more accurately routing flow over road approaches and between subchannels, delineating zones of live-bed sediment transport for use in determining approach channel and bridge channel sections and providing local estimates of hydraulic parameters around piers. All these factors tend to decrease final scour estimates. Two-dimensional models can also provide a clearer picture of hydraulic conditions around bridges during floods, including attack angles that decrease bridge capacity and flow separation zones that can lead to local erosion.

Acknowledgments

Janet Curran assisted with determining flood frequency methods. Mark Henneberg and David Heimann provided insightful comments and corrections during peer review.

References Cited

Arcement, G.J., and Schneider, V.R., 1989, Guide for Selecting Nanning's Roughness Coefficients for Natural Channels and Flood Plains: U.S. Geological Survey Water-Supply Paper 2339, 44 p.

Arneson, L.A., Zevengergen, L.W., Lagasse, P.F., and Clopper, P.E., 2012, Evaluating scour at bridges (5th ed.): Federal Highway Administration Hydraulic Engineering Circular No. 18, Publication No. FHWA-HIF-12-003, 340 p.

Aquaveo, 2018, Surface modeling system 13.0.5: SMS Downloads, accessed November 2018 at https://www.aquaveo.com/downloads-sms?s=SMS&v=13.0.

Beebee, R.A., Dworsky, K.L., and Knopp, S.J., 2017, Streambed scour evaluations and conditions at selected bridge sites in Alaska, 2013-2015: U.S. Geological Survey Scientific Investigations Report 2017-5149, accessed July, 2018, at https://pubs.er.usgs.gov/publication/sir20175149.

Beebee, R.A., and Schauer, P.V., 2015, Streambed scour evaluations and conditions at selected bridge sites in Alaska, 2012: Scientific Investigations Report 2015-5154, 45 p., accessed July, 2018 at https://doi.org/10.3133/sir20155154.

Bergendahl, B.S., and Arneson, L.A., 2014, FHWA hydraulic toolbox (version 4.2): Federal Highway Administration, accessed February 4, 2015, at http://www.fhwa.dot.gov/engineering/hydraulics/software/toolbox404.cfm.

Brunner, G.W., 2016, HEC-RAS—River analysis system hydraulic reference manual (version 5.0): Davis, California, U.S. Army Corps of Engineers Hydrologic Engineering Center, CDP-69, 539 p.

Burgess, M., and Moore, C., Arup, Sydney, 2016, Scour at complex bridge structures–The benefits of two-dimensional hydraulic modelling in the estimation of scour depths: Proceedings of the 2016 Floodplain Management Association National Conference.

Chow, V.T., 1959, Open-channel hydraulics: New York, McGraw-Hill, p. 98–123.

Conaway, J.S., 2004, Summary and comparison of multiphase streambed scour analysis at selected bridge sites in Alaska: U.S. Geological Survey Scientific Investigations Report 2004–5066, 34 p., access June, 2018 at https://doi.org/10.3133/sir20045066.

Conaway, J.S., 2007, Analysis of real-time streambed scour data from bridges in Alaska, in World Environmental and Water Resources Congress, May 15–19, 2007, Tampa, Florida: Proceedings of the American Society of Civil Engineers, 11 p., accessed July, 2018, at https://doi.org/10.1061/40927(243)373.

Conaway, J.S., and Schauer, P.V., 2012, Evaluation of streambed scour at bridges over tidal waterways in Alaska: U.S. Geological Survey Scientific Investigations Report 2012–5245, 38 p., accessed June, 2018, at https://doi.org/10.3133/sir20125245.

Curran, J.H., Barth, N.A., Veilleux, A.G., and Ourso, R.T., 2016, Estimating flood magnitude and frequency at gaged and ungaged sites on streams in Alaska and conterminous basins in Canada, based on data through water year 2012: U.S. Geological Survey Scientific Investigations Report 2016–5024, 47 p., accessed March, 2017, at https://doi.org/10.3133/sir20165024.

England, J.F., Cohn, T.A., Faber, B.A., Stedinger, J.R., Thomas, W.O., Veilleaux, A.G., Kiang, J.E., and Mason, R.R., 2018, Guidelines for determining flood flow frequency bulletin 17C: U.S. Geological Survey Techniques and Methods, book 4, chap B5, 148 p.

Ettema, R., Nakato, T., and Muste, M., 2010, Estimation of scour depth at bridge abutments: Washington, D.C., Transportation Research Board, NCHRP 24-20, 436 p.

Federal Emergency Management Agency, 2011, Flood insurance rate map panel 8110: Federal Emergency Management Agency, Matanuska-Susitna Borough, Alaska, Map Number 02170C8110E.

H.D.R., Inc, 2006, Little Susitna River at Shorty Street emergency enspection report: H.D.R., Inc., Prepared for the Matanuska-Susitna Borough, 8 p.

Heinrichs, T.A., Kennedy, B.W., Langley, D.E., and Burrows, R.L., 2001, Methodology and estimates of scour at selected bridge sites in Alaska: U.S. Geological Survey Water-Resources Investigations Report 00–4151, 44 p.

Hicks, D.M., and Mason, P.D., 1998, Roughness characteristics of New Zealand rivers: Christchurch, New Zealand, National Institute of Water and Atmospheric Research, Ltd., 329 p.

Lagasse, P.F., Zevenbergen, L.W., Spitz, W.J., and Arneson, L.A., 2012, Stream stability at highway structures (4th ed.): Federal Highway Administration Hydraulic Engineering Circular No. 20, Publication No. FHWA-HIF-12-004, 328 p.

Lai, Y.G., 2008, SRH-2D version 2—Theory and user's manual: U.S. Bureau of Reclamation, 109 p.

Norman, V.W., 1975, Scour at selected bridge sites in Alaska: U.S. Geological Survey Water-Resources Investigations Report 32–75, 160 p.

Shan, H., Kilgore, R., Shen, J., and Kerenyi, K., 2016, Updating HEC-18 Pier Scour Equations for Noncohesive Soils: Federal Highway Administration Publication No. FHWA-HRT-16-045, 32 p

Shan, H., Xie, Z., Bojanowski, C., Suaznabar, O., Lottes, S., Shen, J., and Kerenyi, K., 2012, Submerged flow bridge scour under clear water conditions: Federal Highway Administration Publication No. FHWA-HRT-12-034. 43 p.

Turnipseed, D.P., and Sauer, V.B., 2010, Discharge measurements at gaging stations: U.S. Geological Survey Techniques and Methods book 3, 87 p.

U.S. Department of Transportation, Federal Highway Administration, 1988, Scour at bridges: U.S. Department of Transportation, Technical Advisory T5140.20, updated by Technical Advisory T5140.23.

Veilleux, A.G., Cohn, T.A., Flynn, K.M., Mason, R.R., and Hummel, P.R., 2013, Estimating magnitude and frequency of floods using the PeakFQ 7.0 program: U.S. Geological Survey Fact Sheet 2013-3108, 2 p., accessed February 5, 2015, at https://doi.org/10.3133/fs20133108.

Zevenbergen, W., Arneson, L.A., Hunt, J.A., and Miller, A.C., 2012, Hydraulic design of safe bridges: Federal Highway Administration Publication No. FHWA-HIF-12-018, 280 p.

Glossary

Aggradation General and progressive buildup of the longitudinal profile of a channel bed resulting from sediment deposition.

Annual Exceedance Probability (AEP) Flood Annual exceedance probability of a peak flow is the probability of that flow being equaled or exceeded in a 1-year period. It is expressed as a decimal fraction less than 1.0. The recurrence interval of a peak flow is the number of years, on average, in which the specified flow is expected to be equaled or exceeded one time. Exceedance probability and recurrence interval are mathematically inverse of each other; thus, an exceedance probability of 0.01 is equivalent to a recurrence interval of 100 years.

Check Flood A theoretical flood larger than the design flood used by engineers to evaluate hydraulic conditions at a structure. For bridges over waterways, this usually is a 0.2-percent AEP flow (also known as a 500-year recurrence-interval flood).

Design Flood A theoretical flood used by engineers to design a structure. Most bridges are designed to safely withstand the hydraulics created by a 1-percent AEP flow (also known as a 100-year recurrence interval flood).

Low Chord The lowest elevation of the superstructure of a bridge, usually the bottom of the girder supporting the deck or the lowest element of the deck if there is no girder. Also called "low steel."

Superstructure The elements of a bridge, including deck, railing, and girder, that sit on top of the piers and abutments.

Appendix 1. Stream Stability Cross Sections

Repeat cross sections at each bridge, as measured by the Alaska Department of Transportation and Public Facilities and the U.S. Geological Survey, are available for download at https://doi.org/10.3133/sir20195110.

Publishing support provided by the U.S. Geological Survey
Science Publishing Network, Tacoma Publishing Service Center

For more information concerning the research in this report, contact the
Director, Alaska Science Center
U.S. Geological Survey
4210 University Drive
Anchorage, Alaska 99508
https://www.usgs.gov/centers/asc/

ISSN 2328-0328 (online)
https://doi.org/10.3133/sir20195110